Supporting information

Ruthenium-vinylhelicenes: remote metal-based enhancement and redox switching of the chiroptical properties of a helicene core

Emmanuel Anger, Monika Srebro, Nicolas Vanthuyne, Loïc Toupet, Christian Roussel, Stéphane Rigaut, Jochen Autschbach, Jeanne Crassous,* and Régis Réau**

Institut des Sciences Chimiques de Rennes, UMR 6226, Institut de Physique de Rennes, UMR 6251, Campus de Beaulieu, CNRS-Université de Rennes 1, 35042 Rennes Cedex, France

Department of Chemistry, University of Buffalo, State University of New York,Buffalo, NY 14260-3000, USA

Faculty of Chemistry, Jagiellonian University, 30-060 Krakow, Poland.

Chirosciences, UMR 7313, Stéréochimie Dynamique et Chiralité, Aix-Marseille University, 13397 Marseille Cedex 20, France

Full reference 2b: Sehnal, P. ; Stara, I.G.; Saman, D., Tichy, M.; Misek, J.; Cvacka, J.; Rulisek, L.; Chocholousova, J.; Vacek, J.; Goryl, G.; Szymonski, M.; Cisarova, I.; Stary, I. *PNAS* **2009**, *106*, 13169-13174.

Full reference 10b: Adriaenssens, L.; Severa, L.; Salova, T. ; Cisarova, I. ; Pohl, R. ; Saman, D. ; Rocha, S. V. ; Finney, N. S.; Pospisil, L.; Slavicek, P.; Teply, F. *Chem. Eur. J.* **2009**, *15*, 1072-1076.

Experimental section

All experiments were performed under an atmosphere of dry argon using standard Schlenk techniques. Commercially available reagents were used as received without further purification. Solvents were freshly distilled under argon from sodium/benzophenone (tetrahydrofuran, diethyl ether) or from phosphorus pentoxide (pentane, dichloromethane). Irradiation reactions were conducted using a Heraeus TQ 150 mercury vapor lamp. Preparative separations were performed by gravity column chromatography on basic alumina (Aldrich, Type 5016A, 150 mesh, 58 Å) or silica gel (Merck Geduran 60, 0.063-0.200 mm) in 3.5-20 cm columns. ^{1}H, ^{13} C, and ^{31} P NMR spectra were recorded on a BrukerAM300, AV400 or AV500. ^{1}H and ^{13}C NMR chemical shifts were reported in parts per million (ppm) relative to Me_4Si as external standard. ^{31}P NMR downfield chemical shifts were expressed with a positive sign, in ppm, relative to external 85% H_3PO_4 and were decoupled from the proton. Assignment of proton atoms is based on COSY experiment. Assignment of carbon atoms is based on HMBC, HMQC and DEPT-135 experiments. High-resolution mass spectra were obtained on a Varian MAT 311 or ZabSpec TOF Micromass instrument at CRMPO, University of Rennes 1. Elemental analyses were performed by the CRMPO, University of Rennes 1. Specific rotations (in deg cm^2 g^{-1}) were measured in a 1 dm thermostated quartz cell on a Perkin Elmer-341 polarimeter. Circular dichroism (in M^{-1} cm^{-1}) was measured on a JascoJ-815 Circular Dichroism Spectrometer (IFR140 facility - Université de Rennes 1), adapted with an extended wavelength option to 1100nm for NIR-CD.UV/vis/NIR spectroscopy was conducted on a Varian Cary 5000 spectrometer.

Benzo[c]phenanthrylmethylphosphoniumbromide [1], naphtyl-2,7-dimethylphosphoniumbromide [2], 4-[(trimethylsilyl)-ethynyl]benzaldehyde [3], 4-ethynylbenzaldehyde[3] and $RuHClCO(P^iPr_3)_2$ [4] were prepared according to literature procedures.

2-Ethynyl-carbo[6]helicene (±)-1a.

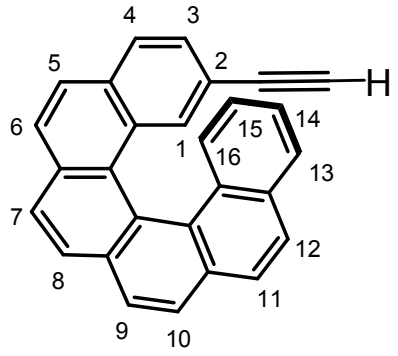

1) *Synthesis of2-[2-(4-ethynylphenyl)ethenyl]benzo[c]phenanthrene*. To a stirred suspension of benzo[c]phenanthrylmethylphosphonium bromide [1] (900mg , 1.54mmol) in anhydrous THF (20mL) cooled to -78°C under argon, was added dropwise *n*-BuLi 1.6 M in hexanes (0.96 mL, 1.54 mmol). The reaction mixture was warmed to room temperature and stirred for 30 min. Then the reaction mixture was cooled to -78°C and a solution of 4-ethynylbenzaldehyde (220 mg, 1.54 mmol) in anhydrous THF (10 mL) was added dropwise. After stirring under argon at room temperature for three hours, the reaction mixture was filtered over Celite. Evaporation of the solvent and column chromatography over silica gel (using heptane / EtOAc 8:2 as eluent) afforded a yellow solid (500 mg, 90%) as a *Z*/*E* isomeric mixture. Rf (heptane / EtOAc 8:2) 0.7. ^{1}H NMR (300 MHz, $CDCl_3$) δ9.20 (d, J = 8.3 Hz, 1H), 9.12 (s, 1H), 9.03 (s, 0.7H), 8.56 (d, J = 8.5 Hz, 0.7H), 8.10 (d, J = 7.6 Hz, 1.3H), 8.04 (d, J = 7.8 Hz, 1H), 7.95 (d, J = 8.5 Hz, 3.5H), 7.91-7.87 (m, 1.4H), 7.82 (m, 6.7H), 7.72 (dd, J = 15.0, 7.3 Hz, 2.4H), 7.62 (m, 3.5H), 7.59-7.52 (m, 3.5H), 7.49 (d, J = 7.9 Hz, 1.8H), 7.21 (d, J = 16.3 Hz, 1.3H), 7.34 (d, J = 16.3 Hz, 1.1H), 6.75 (d, J = 12.1 Hz, 0.6H), 6.93 (d, J = 12.1Hz, 0.6H), 3.34 (s, 0.9H), 3.25 (s, 0.6H). ^{13}C NMR (75 MHz, $CDCl_3$) δ138.2 (*C*), 138.0 (*C*), 135.0 (*C*), 134.8 (*C*), 133.7 (*C*), 133.5 (*C*), 133.3 (*C*), 132.70 (*C*), 132.6 (*C*H), 132.4 (*C*H), 132.1 (*C*H), 131.5 (*C*), 131.3 (*C*), 130.7 (*C*), 130.6 (*C*), 130.4 (*C*H), 130.3 (*C*), 130.0 (*C*H), 129.4 (*C*H), 129.1 (*C*H), 128.9 (*C*H), 128.6 (*C*H), 128.5 (*C*H), 128.2 (*C*H), 127.9 (*C*H), 127.7 (*C*H), 127.7 (*C*H), 127.6 (*C*H), 127.5 (*C*), 127.4 (*C*), 127.2 (*C*H), 127.2 (*C*), 127.2 (*C*H), 127.0 (*C*H), 126.9 (*C*H), 126.7 (*C*H), 126.6 (*C*H), 126.4 (*C*H), 126.0 (*C*H), 123.2 (*C*H), 121.1 (*C*), 121.0 (*C*), 84.1 (*C*H), 83.9 (*C*H), 78.4 (*C*H), 78.1 (*C*H).

2) *Synthesis of 2-ethynyl-carbo[6]helicene (±)-**1a***. 2-[2-(4-Ethynylphenyl)ethenyl]benzo[c]phenanthrene (250 mg, 0.75 mmol) in 700mL of toluene was irradiated for one night in the presence of catalytic quantities of iodine using Heraeus TQ 150 mercury vapor lamp. Then the solvent was stripped off and the crude product was purified by column chromatography (silica gel, heptane) to give 100 mg (0.3mmol, 40%) of 2-ethynyl-carbo[6]helicene (±)-**1a** as a yellow solid. Rf (heptane) 0.20. ^{1}H NMR (500 MHz, C*D*Cl_3) δ 8.06-8.02 (m, 3H), 8.01-7.95 (m, 4H), 7.92-7.87 (m, 2H, H^{helix} and H^{13}), 7.81 (s, 1H, H^{1}), 7.79 (d, $^{3}J_{H\text{-}H}$ = 8.2 Hz, 1H, H^{4}), 7.59 (d, $^{3}J_{H\text{-}H}$ = 8.5 Hz, 1H, H^{16}), 7.34-7.30 (m, 2H, H^{3} and H^{14}), 6.78-6.72 (m, 1H, H^{15}), 2.74 (s, 1H, ≡C*H*). ^{13}C NMR (126 MHz, C*D*Cl_3) δ 133.2 (*C*), 132.5 (*C*H), 132.2 (*C*), 131.5 (*C*), 131.5 (*C*), 129.5 (*C*), 129.4 (*C*), 128.3 (*C*H), 128.1 (*C*H), 127.8 (*C*H), 127.7 (*C*), 127.6 (*C*H), 127.5 (*C*Hx2), 127.45 (*C*), 127.4 (*C*x2), 127.35 (*C*), 127.3 (*C*H), 127.1 (*C*H), 126.9 (*C*H), 126.1 (*C*H), 125.8 (*C*H), 124.7 (*C*H), 123.9 (*C*), 118.25 (*C*), 83.7 (*C*H), 76.1 (≡*C*H).HRMS (EI) calcd for $C_{28}H_{16}$, $[M+Na]^{+}$**:** 375.11497; found: 375.1150. Elemental analysis, calcd. (%) for $C_{28}H_{16}$: C 95.42, H 4.58; found : C 95.34, H 4.67.UV/Vis (6.8 10^{-5} M, CH_2Cl_2): 323 (26000), 329 (23500), 352 (12940), 391 (660), 413 (360).

Complex (±)-2a.

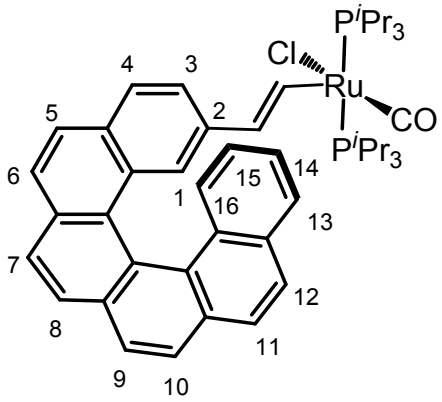

To a solution of 2-ethynylcarbo[6]helicene (±)-**1a** (20 mg, 0.05 mmol) in 2mL of CH_2Cl_2 under argon was added RuHClCO(P^iPr_3)$_2$ [4] (27mg, 0.05mmol) and the reaction mixture was stirred for 30 min. at room temperature. Dark red single crystals of (±)-**2a** (37 mg, 90%) were then grown upon slow evaporation under argon. ^{1}H NMR (400 MHz, C*D*Cl$_3$) δ 8.36 (d, $^3J_{H\text{-}H}$= 13.3 Hz, 1H, RuC*H*=CH), 7.99-7.89 (m, 6H), 7.84 (d, $^3J_{H\text{-}H}$= 8.5 Hz, 1H), 7.79 (d, $^3J_{H\text{-}H}$ = 8.5 Hz, 1H), 7.76 (dd, *J* = 8.00, 1.03 Hz, 1H, H^{13}), 7.70 (d, $^3J_{H\text{-}H}$ = 8.1 Hz, 1H, H^{16}), 7.66 (d, $^3J_{H\text{-}H}$ = 8.4 Hz, 1H, H^4), 7.23 (dd, $^3J_{H\text{-}H}$= 8.5 Hz, $^4J_{H\text{-}H}$= 1.6 Hz, 1H, H^3), 7.20-7.13 (m, 1H, H^{14}), 7.00 (s, 1H, H^1), 6.72 (ddd, *J* = 8.4, 6.9, 1.35 Hz, 1H, H^{15}), 5.26 (dt, $^3J_{H\text{-}H}$= 13.4 Hz, $^3J_{P\text{-}H}$= 2.1 Hz, 1H, RuCH=C*H*), 2.70 (sext, *J* = 7.1 Hz, 3H, PC*H*), 2.60 (sext, *J* = 7.1 Hz, 3H, PC*H*), 1.34-1.24 (m, 18H, PCH(CH_3)$_3$), 1.18-1.04 (m, 18H, PCH(CH_3)$_3$). ^{31}P NMR (162 MHz, C*D*Cl$_3$) δ 39.39 (d, $^3J_{P\text{-}P}$= 275 Hz), 37.40 (d, $^3J_{P\text{-}P}$ = 275 Hz).^{13}C NMR (101 MHz, C*D*Cl$_3$) δ 202.6 (t, $^2J_{P\text{-}C}$= 13 Hz, *C*O), 150.6 (t, $^2J_{P\text{-}C}$ = 10.7 Hz, Ru*C*H=CH), 135.5 (*C*), 134.4 (t, $^3J_{P\text{-}C}$ = 3 Hz, RuCH=*C*H), 132.8 (*C*), 131.7 (*C*), 131.5 (*C*), 131.0 (*C*), 130.7 (*C*), 129.9 (*C*), 129.2 (*C*), 128.2 (*C*), 128.1 (*C*), 127.7 (*C*H), 127.6 (*C*Hx2), 127.4 (*C*H), 127.3 (*C*H), 127.2 (*C*H), 126.9 (*C*H), 126.6 (*C*H), 126.4 (*C*H), 126.2 (*C*H), 125.3 (*C*H), 124.5 (*C*H), 124.2 (*C*), 124.1 (*C*H), 122.9 (*C*H), 122.1 (*C*H), 24.57-23.96 (*C*H ^{i}Pr x 6), 19.94 (*C*H$_3$^{i}Pr x 3), 19.90 (*C*H$_3$^{i}Pr x 3), 19.81 (*C*H$_3$^{i}Pr x 3), 19.56 (*C*H$_3$^{i}Pr x 3). Elemental analysis, calcd. (%) for $C_{47}H_{59}ClOP_2Ru$: C 67.33, H 7.09; found: C 66.89, H 7.30.UV/Vis (2.4 10^{-5} M, CH_2Cl_2): 318 (36600), 334 (25500), 342 (22000), 350 (19350), 390 (11300), 530 (690).

2,15-Diethynyl-carbo[6]helicene (±)-1b.

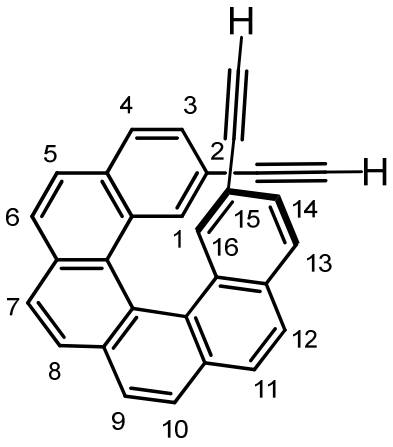

1) *Synthesis of* 2,7-*[2-(4-((trimethylsilyl)ethynyl)phenyl)ethenyl]naphtalene*. To a stirred suspension of naphtyl-2,7-dimethylphosphonium bromide [2] (1g , 1.2mmol) in anhydrous THF (40mL) cooled to -78°C under argon, was added dropwise *n*-BuLi 1.6 M in hexanes (1.55 mL, 2.4mmol). The reaction mixture was warmed to room temperature and

stirred for 30 min. Then the reaction mixture was cooled to -78°C and a solution of 4-((trimethylsilyl)ethynyl)benzaldehyde [3] (485 mg, 2.4mmol) in anhydrous THF (5 mL) was added dropwise. After stirring under argon at room temperature for three hours, the reaction mixture was filtered over Celite. Evaporation of the solvent and column chromatography over silica gel (using heptane / EtOAc 8:2 as eluent) afforded 385 mg of a yellow solid (0.73 mmol, 60%), Rf (heptane / EtOAc 8:2) 0.4-0.5, which was used directly as an isomeric mixture for the next step.

2) *Synthesis of 2,7-bis((trimethylsilyl)ethynyl)-carbo[6]helicene.* 2,7-Bis[2-(4-((trimethylsilyl)ethynyl)phenyl)-ethenyl]naphtalene (190 mg, 0.36mmol) in 700mL of toluene was irradiated for one night in the presence of catalytic quantities of iodine using Heraeus TQ 150 mercury vapor lamp. Then the solvent was stripped off and the crude product was purified by column chromatography (silica gel, heptane) to give 75 mg (0.14 mmol, 40 %) of 2,7-bis((trimethylsilyl)ethynyl)-carbo[6]helicene as a yellow solid. Rf (heptane / EtOAc 8:2) 0.4. NMR (500 MHz, $CDCl_3$) δ 8.02 (d, J = 8.2 Hz, 2H), 7.98 (d, J = 8.2 Hz, 2H), 7.96 (d, J = 8.5 Hz, 2H), 7.90 (d, J = 8.5 Hz, 2H), 7.79-7.74 (m, 4H), 7.36 (dd, J = 8.3,1.5 Hz, 1H), 7.35 (d, J = 1.47 Hz, 1H), 0.20 (s, 18H).^{13}C NMR (75 MHz, CD_2Cl_2) δ133.3 (*C*), 132.2 (*C*H), 131.8 (*C*), 128.9 (*C*), 127.85 (*C*H), 127.8 (*C*H), 127.4 (*C*H), 127.35 (*C*H), 127.3 (*C*H), 127.30 (*C*H), 127.0 (*C*), 123.8 (*C*), 119.2 (*C*), 105.1 (*C*), 93.4 (*C*), -0.47 (*C*H_3x6). Elemental analysis, calcd. (%) for $C_{36}H_{32}Si_2$: C 83.02, H 6.19; found : C 82.76, H 6.57.

3) *Synthesis of 2,7-bis(ethynyl)-carbo[6]helicene (±)-**1b**.2,7-bis((trimethylsilyl)ethynyl)-carbo[6]helicene* [5]. (145 mg, 0.28mmol) and K_2CO_3 (35mg, 0.25 mmol) in 30 mL of a mixture CH_2Cl_2/MeOH (1/1) was stirred for one night. After evaporation, the crude product was extracted using CH_2Cl_2 and water. Organic layer was dried over $MgSO_4$ then evaporated to give 100 mg (0.27 mmol, 99 %) of 2,7-bis(ethynyl)-carbo[6]helicene (±)-**1b** as a yellow solid. Rf (heptane / EtOAc 8:2) 0.20. ^{1}H NMR (500 MHz, $CDCl_3$) δ 8.05 (d, J = 8.2 Hz, 2H), 8.01 (d, J = 8.2 Hz, 2H), 7.99 (d, J = 8.5 Hz, 2H), 7.94 (d, J = 8.5 Hz, 2H), 7.81 (d, J = 8.2 Hz, 2H), 7.75 (ls, 2H), 7.36 (dd, J = 8.2, 1.5 Hz, 2H), 2.73 (s, 2H). ^{13}C NMR (126 MHz, C*D*Cl_3) δ 133.7 (*C*), 132.3 (*C*), 132.25 (*C*H), 132.2 (*C*), 129.5 (*C*), 128.8 (*C*H), 128.3 (*C*H), 127.9 (*C*H), 127.8 (*C*H), 127.4 (*C*), 124.1 (*C*), 118.6 (*C*), 83.8 (*C*H), 76.6 (≡*C*H). HRMS (EI), calcd. (%) for $C_{30}H_{16}$: 376.1252; found :376.1273. Elemental analysis, calcd. (%) for $C_{30}H_{16}$: C 95.72, H 4.28; found : C 95.54, H 4.27. UV/Vis (5.3 10^{-5} M, CH_2Cl_2): 326 (21540), 336 (18500), 355 (11000), 394 (670), 417 (380).

Complex (±)-2b.

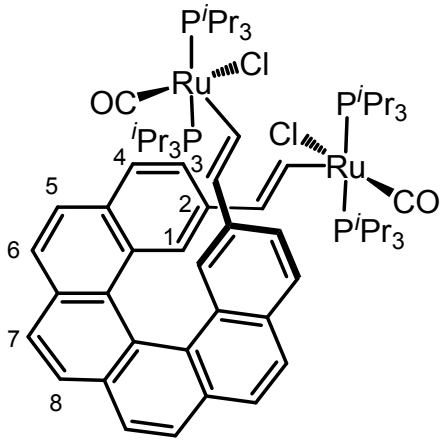

To a solution of 2,15-diethynylcarbo[6]helicene[5] (±)-**1b** (20 mg, 0.05 mmol) in 2 mL of CH_2Cl_2 under argon was added RuHClCO(P^{i}Pr$_3$)$_2$ [4] (50 mg, 0.1mmol) and the reaction mixture was stirred for 30 min. at room temperature. Dark red single crystals of (±)-**2b** (56 mg, 80%) were then grown upon slow evaporation under argon. ^{1}H NMR (300 MHz, CD_2Cl_2) δ 8.21 (d, $^3J_{H\text{-}H}$= 13.3 Hz, 2H, RuC*H*=CH), 7.82 (s, 4H), 7.69 (s, 4H), 7.47 (d, $^3J_{H\text{-}H}$ = 8.4 Hz, 2H, H^4), 7.07 (dd, J = 8.4, 1.3 Hz, 2H, H^3), 6.90 (s, 2H, H^1), 5.16 (dt, $^3J_{H\text{-}H}$= 13.4 Hz, $^3J_{P\text{-}H}$= 2.1 Hz, 2H, RuCH=C*H*), 2.58 (sext, J =

7.1 Hz, 6H, PC*H*(CH_3)$_3$), 2.48 (sext, *J* = 7.1 Hz, 6H, PC*H*(CH_3)$_3$), 1.34-1.24 (m, 36H, PCH(C*H*$_3$)$_3$), 1.18-1.04 (m, 36H, PCH(C*H*$_3$)$_3$).^{31}P NMR (162 MHz, C*D*$_2$Cl$_2$) δ 39.2 (d, $^3J_{P-P}$= 275 H), 36.48 (d, $^3J_{P-P}$ = 275 Hz). ^{13}C NMR (75 MHz, C*D*$_2$Cl$_2$) δ 203.1 (t, $^2J_{P-C}$= 13.2 Hz, *C*O), 150.6 (t, $^2J_{P-C}$ = 10.9 Hz, Ru*C*H=CH), 135.5 (*C*), 135.1 (t, $^3J_{P-C}$ = 3.3 Hz, RuCH=*C*H), 132.8 (*C*), 131.5 (*C*), 131.1 (*C*), 129.5 (*C*), 128.6 (*C*), 128.0 (*C*H), 127.8 (*C*H), 127.2 (*C*H), 126.3 (*C*H), 124.5 (*C*), 124.4 (*C*H), 122.6 (*C*H), 122.3 (*C*H), 24.9, 24.8, 24.7, 24.6, 24 .5, 24.4 (*C*H ^{i}Pr), 20.2, 20.1, 20.0, 19.7 (*C*H$_3$^{i}Pr).Elemental analysis, calcd. (%) for $C_{68}H_{102}Cl_2O_2P_4Ru_2$: C 60.57, H 7.62; found : C 58.98, H 8.02. UV/Vis (2.5 10^{-5} M, CH_2Cl_2): 314 (47400), 330 (43120), 345 (33320), 382 (21600), 344 (4830), 517 (840).

Figure S1. 500 MHz ^{1}H NMR ($CDCl_3$, 298K) of complex **2a**.

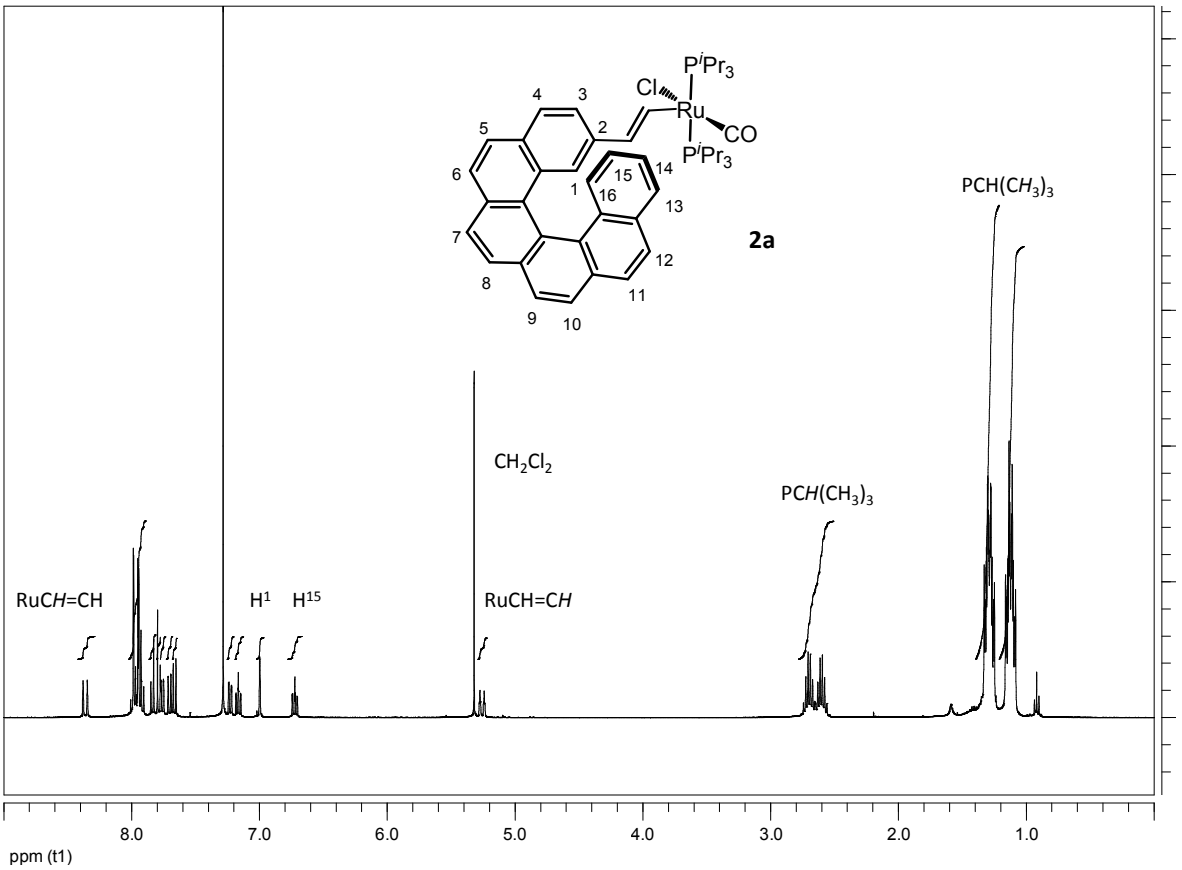

Figure S2. 500 MHz ^{1}H NMR ($CDCl_3$, 298K) of complex **2b**.

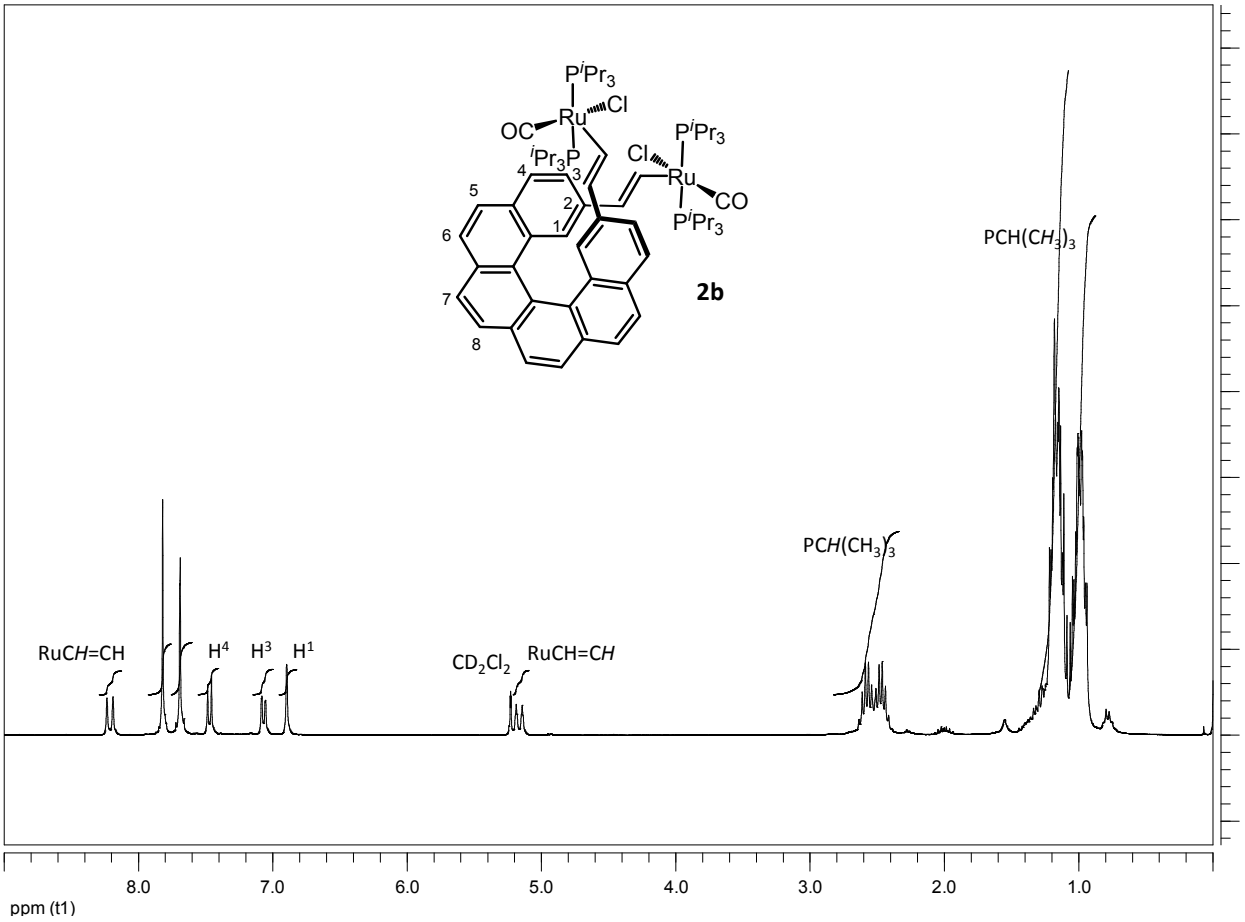

Figure S3. UV-vis spectra of **1a**, **2a**, **1b** and**2b** in CH_2Cl_2(*C* 1-5 10^{-5} M^{-1})

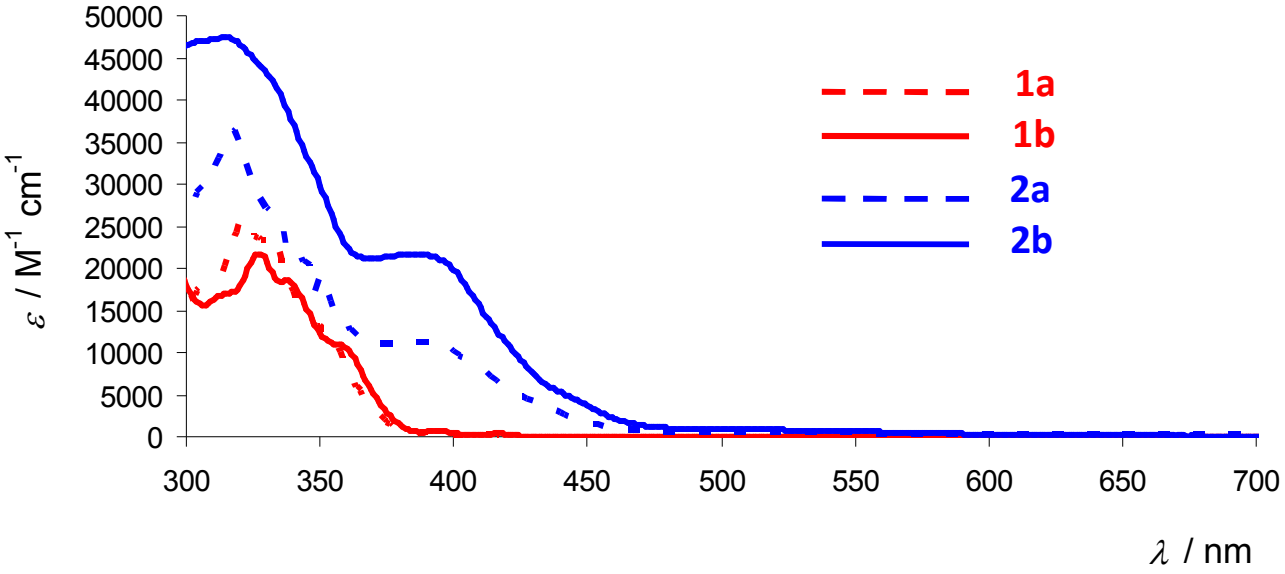

X-ray Crystallographic Studyof 2a and 2b

Single crystals suitable for X-Ray crystal analysis were obtained by slow diffusion of pentane vapors into a dichloromethane solution of **2a** and **2b** at room temperature. Single crystal data collection were performed at 140 or 150 K with an APEX II Bruker-AXS (Centre de Diffractométrie, Université de Rennes 1, France) with Mo-*K*α radiation (λ = 0.71069 Å)Reflections were indexed, Lorentz-polarization corrected and integrated by the *DENZO* program of the KappaCCD software package. The data merging process was performed using the SCALEPACK program [6]. Structure determinations were performed by direct methods with the solving program SIR97, [7] that revealed all the non hydrogen atoms. SHELXL program [8] was used to refine the structures by full-matrix least-squares based on F^2. All non-hydrogen atoms were refined with anisotropic displacement parameters. Hydrogen atoms were included in idealised positions and refined with isotropic displacement parameters.

Atomic scattering factors for all atoms were taken from International Tables for X-ray Crystallography [9]. Details of crystal data and structural refinements are given in Table S1. CCDC reference numbers 808470, 855106 contain the supplementary crystallographic data for this paper. These data can be obtained free of charge at www.ccdc.cam.ac.uk/conts/retreving.html or from the Cambridge Crystallographic Data Center, 12 union Road, Cambridge CB2 1EZ, UK; Fax: (internat.) + 44-1223-336-033; E-mail: deposit@ccdc.cam.ac.uk].

Figure S4. ORTEP plot of the molecular structure of (P^iPr_3)$_2$(CO)ClRu(CH=CH−[6]helicene) (**2a**).

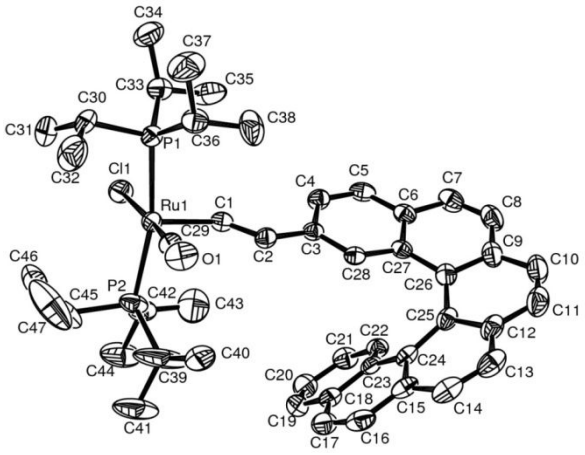

Table S1. Crystal data and structure refinement for $(P^iPr_3)_2(CO)ClRu(CH{=}CH{-}[6]helicene)$ (**2a**).

Empirical formula	$C_{47}H_{59}ClOP_2Ru$
Formula weight	838.40
Temperature	163(2) K
Wavelength	0.71073 Å
Crystal system	Triclinic
Space group	P-1
Unit cell dimensions	a = 10.8723(3) Å α = 83.887(3) deg.
	b = 13.9019(5) Å β = 78.634(2) deg.
	c = 14.4817(4) Å γ = 86.384(3) deg.
Volume	2131.73(11) $Å^3$
Z	2
Calculated density	1.306 Mg/m^3
Absorption coefficient	0.539 mm^{-1}
F(000)	880
Crystal size	0.24 x 0.18 x 0.09 mm
θ range for data collection	2.61 to 27.00 deg.
Index ranges	-13<=h<=11, -17<=k<=16, -18<=l<=12
Reflections collected	15463
Independent reflexions	9157 [R(int) = 0.0254]
Completeness to θ	0.986
Refinement method	Full-matrix least-squares on F^2
Data / restraints / parameters	9157 / 0 / 470
Goodness-of-fit on F^2	0.906
Final R indices [I>2σ(I)]	R1 = 0.0409, wR2 = 0.0866
R indices (all data)	R1 = 0.0685, wR2 = 0.0984
Extinction coefficient	0.0026(4)
Largest diff. peak and hole	0.862 and -0.646 $e.Å^{-3}$

Table S2. Bond lengths [A] and angles [deg] for (P^iPr_3)$_2$(CO)ClRu(CH=CH−[6]helicene) (**2a**).

Ru(1)-C(29)	1.837(4)	C(29)-Ru(1)-Cl(1)	173.69(10)
Ru(1)-C(1)	1.981(3)	C(1)-Ru(1)-Cl(1)	94.49(8)
Ru(1)-P(1)	2.4028(9)	P(1)-Ru(1)-Cl(1)	88.62(3)
Ru(1)-P(2)	2.4071(9)	P(2)-Ru(1)-Cl(1)	88.02(3)
Ru(1)-Cl(1)	2.4285(8)	C(33)-P(1)-C(36)	110.21(15)
P(1)-C(33)	1.853(3)	C(33)-P(1)-C(30)	103.24(16)
P(1)-C(36)	1.858(3)	C(36)-P(1)-C(30)	102.89(15)
P(1)-C(30)	1.863(3)	C(33)-P(1)-Ru(1)	115.59(11)
P(2)-C(39)	1.840(4)	C(36)-P(1)-Ru(1)	115.97(12)
P(2)-C(42)	1.842(3)	C(30)-P(1)-Ru(1)	107.24(11)
P(2)-C(45)	1.856(4)	C(39)-P(2)-C(42)	107.4(3)
O(1)-C(29)	1.090(4)	C(39)-P(2)-C(45)	102.8(3)
C(1)-C(2)	1.336(4)	C(42)-P(2)-C(45)	104.41(16)
C(1)-H(1)	0.9500	C(39)-P(2)-Ru(1)	119.03(14)
C(2)-C(3)	1.464(4)	C(42)-P(2)-Ru(1)	115.48(11)
C(2)-H(2)	0.9500	C(45)-P(2)-Ru(1)	105.94(15)
C(3)-C(28)	1.376(4)	C(2)-C(1)-Ru(1)	135.8(2)
C(3)-C(4)	1.423(4)	C(1)-C(2)-C(3)	126.6(3)
C(4)-C(5)	1.357(4)	C(28)-C(3)-C(4)	117.8(3)
C(4)-H(4)	0.9500	C(28)-C(3)-C(2)	119.7(2)
C(5)-C(6)	1.409(4)	C(4)-C(3)-C(2)	122.5(3)
C(5)-H(5)	0.9500	C(5)-C(4)-C(3)	120.2(3)
C(6)-C(27)	1.424(4)	C(4)-C(5)-C(6)	122.1(3)
C(6)-C(7)	1.428(4)	C(5)-C(6)-C(27)	119.1(3)
C(7)-C(8)	1.335(5)	C(5)-C(6)-C(7)	122.2(3)
C(7)-H(7)	0.9500	C(27)-C(6)-C(7)	118.6(3)
C(8)-C(9)	1.422(5)	C(8)-C(7)-C(6)	120.9(3)
C(8)-H(8)	0.9500	C(7)-C(8)-C(9)	122.2(3)
C(9)-C(10)	1.415(5)	C(10)-C(9)-C(26)	119.5(3)
C(9)-C(26)	1.421(4)	C(10)-C(9)-C(8)	121.2(3)
C(10)-C(11)	1.344(5)	C(26)-C(9)-C(8)	119.1(3)
C(10)-H(10)	0.9500	C(11)-C(10)-C(9)	121.2(3)
C(11)-C(12)	1.419(4)	C(10)-C(11)-C(12)	120.7(3)
C(11)-H(11)	0.9500	C(11)-C(12)-C(13)	120.8(3)
C(12)-C(13)	1.419(5)	C(11)-C(12)-C(25)	119.5(3)
C(12)-C(25)	1.424(4)	C(13)-C(12)-C(25)	119.7(3)
C(13)-C(14)	1.343(4)	C(14)-C(13)-C(12)	121.2(3)
C(13)-H(13)	0.9500	C(13)-C(14)-C(15)	120.3(3)
C(14)-C(15)	1.416(4)	C(24)-C(15)-C(14)	120.2(3)
C(14)-H(14)	0.9500	C(24)-C(15)-C(16)	120.1(3)
C(15)-C(24)	1.407(4)	C(14)-C(15)-C(16)	119.6(3)
C(15)-C(16)	1.433(4)	C(17)-C(16)-C(15)	121.8(3)
C(16)-C(17)	1.341(4)	C(16)-C(17)-C(18)	120.3(3)
C(16)-H(16)	0.9500	C(19)-C(18)-C(17)	120.6(3)
C(17)-C(18)	1.421(4)	C(19)-C(18)-C(23)	119.2(3)
C(17)-H(17)	0.9500	C(17)-C(18)-C(23)	120.2(3)
C(18)-C(19)	1.414(4)	C(20)-C(19)-C(18)	121.5(3)
C(18)-C(23)	1.425(4)	C(19)-C(20)-C(21)	119.9(3)
C(19)-C(20)	1.352(5)	C(22)-C(21)-C(20)	120.1(3)
C(19)-H(19)	0.9500	C(21)-C(22)-C(23)	121.8(3)
C(20)-C(21)	1.400(4)	C(22)-C(23)-C(18)	117.4(3)
C(20)-H(20)	0.9500	C(22)-C(23)-C(24)	123.7(3)
C(21)-C(22)	1.375(4)	C(18)-C(23)-C(24)	118.8(3)
C(21)-H(21)	0.9500	C(15)-C(24)-C(25)	118.4(2)
C(22)-C(23)	1.407(4)	C(15)-C(24)-C(23)	117.2(3)
C(22)-H(22)	0.9500	C(25)-C(24)-C(23)	124.1(3)
C(23)-C(24)	1.470(4)	C(12)-C(25)-C(26)	117.3(3)
C(24)-C(25)	1.452(4)	C(12)-C(25)-C(24)	116.6(3)
C(25)-C(26)	1.450(4)	C(26)-C(25)-C(24)	126.1(2)
C(26)-C(27)	1.442(4)	C(9)-C(26)-C(27)	117.5(3)
C(27)-C(28)	1.413(4)	C(9)-C(26)-C(25)	117.7(3)
C(28)-H(28)	0.9500	C(27)-C(26)-C(25)	124.6(2)
C(30)-C(31)	1.531(4)	C(28)-C(27)-C(6)	116.7(3)
C(30)-C(32)	1.534(5)	C(28)-C(27)-C(26)	123.4(3)
		C(6)-C(27)-C(26)	119.8(3)
		C(3)-C(28)-C(27)	123.8(3)
C(29)-Ru(1)-C(1)	91.48(13)	O(1)-C(29)-Ru(1)	177.6(3)
C(29)-Ru(1)-P(1)	88.76(10)	C(31)-C(30)-C(32)	110.7(3)
C(1)-Ru(1)-P(1)	95.91(9)	C(31)-C(30)-P(1)	111.2(2)
C(29)-Ru(1)-P(2)	93.38(10)	C(32)-C(30)-P(1)	111.7(3)
C(1)-Ru(1)-P(2)	95.78(9)	C(35)-C(33)-C(34)	110.3(3)
P(1)-Ru(1)-P(2)	168.06(3)	C(35)-C(33)-P(1)	113.5(3)

C(34)-C(33)-P(1)	117.7(3)
C(38)-C(36)-C(37)	110.0(3)
C(38)-C(36)-P(1)	113.1(2)
C(37)-C(36)-P(1)	116.0(3)
C(40)-C(39)-C(41)	117.0(4)
C(40)-C(39)-P(2)	125.4(3)
C(41)-C(39)-P(2)	117.4(3)
C(43)-C(42)-C(44)	109.9(3)
C(43)-C(42)-P(2)	112.4(2)
C(44)-C(42)-P(2)	116.2(3)
C(46)-C(45)-C(47)	110.3(5)
C(46)-C(45)-P(2)	113.7(3)
C(47)-C(45)-P(2)	109.6(3)

Figure S5. Packing of complex **2a** in the crystal.

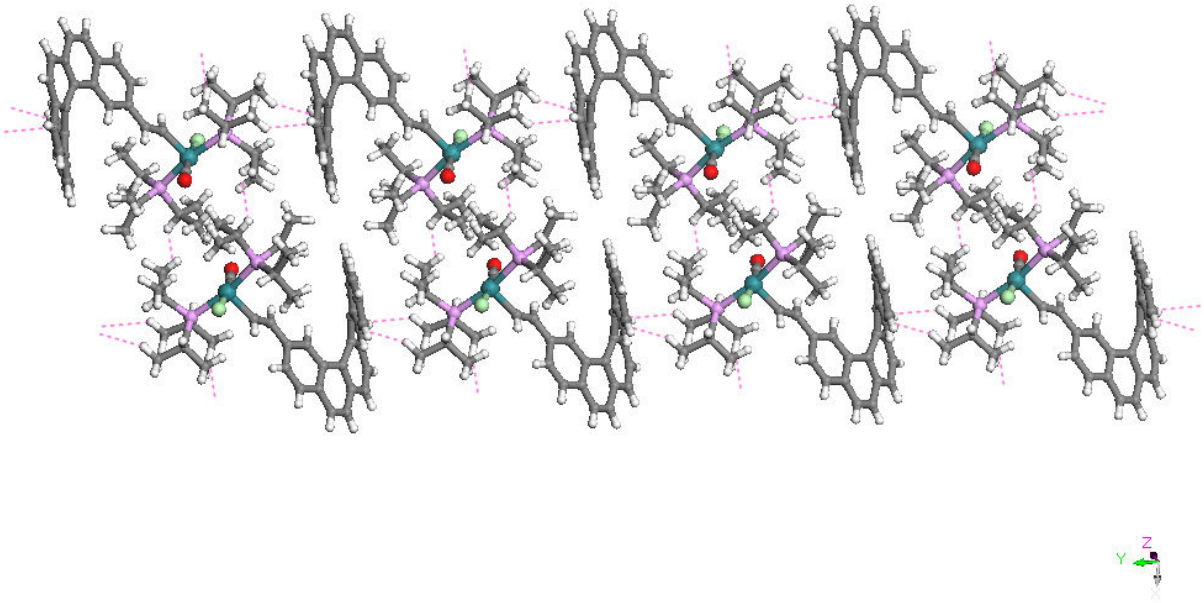

Figure S6. ORTEP plot of the molecular structure of $(P^iPr_3)_2(CO)ClRu(CH=CH\text{-}[6]helicene\text{-}CH=CH)RuCl(CO)(P^iPr_3)_2$ (**2b**).

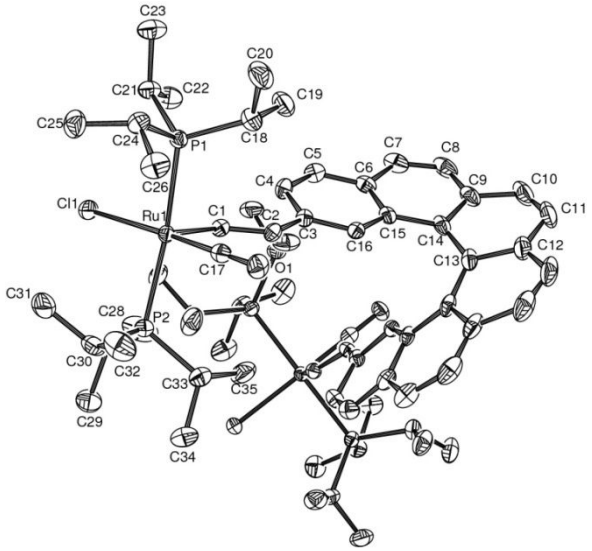

Table S3. Crystal data and structure refinement for **2b**.

Empirical formula	$C_{72}H_{110}Cl_{10}O_2P_4Ru_2$
Formula weight	1688.12
Temperature	120(2) K
Wavelength	0.71073 Å
Crystal system	Monoclinic
Space group	C2/c
Unit cell dimensions	a = 12.1161(2) Åα= 90 deg.
	b = 19.0277(2) Å β = 99.7390(10) deg.
	c = 35.7678(5) Å γ = 90 deg.
Volume	8127.1(2) A^3
Z	4
Calculated density	1.380 Mg/m^3
Absorption coefficient	0.820 mm^{-1}
F(000)	3504
Crystal size	0.286 x 0.251 x 0.062 mm
θrange for data collection	2.75 to 27.00 °
Index ranges	-15<=h<=15, -24<=k<=24, -45<=l<=45
Reflections collected	56651
Independent reflexions	8884 [R(int) = 0.0372]
Completeness to θ= 27.00	0.999
Refinement method	Full-matrix least-squares on F^2
Data / restraints / parameters	8884 / 0 / 407
Goodness-of-fit on F^2	1.030
Final R indices [I>2σ(I)]	R1 = 0.0299, wR2 = 0.0690
R indices (all data)	R1 = 0.0451, wR2 = 0.0719
Largest diff. peak and hole	0.896 and -0.701 $e.Å^{-3}$

Table S4. Bond lengths [A] and angles [deg] for **2b**.

C(41)-Cl(3)	1.747(3)	C(33)-P(2)-Ru(1)	116.01(7)
C(41)-Cl(2)	1.767(3)	C(30)-P(2)-Ru(1)	106.00(7)
C(42)-Cl(5)	1.741(3)	C(2)-C(1)-Ru(1)	134.37(16)
C(42)-Cl(4)	1.748(3)	C(1)-C(2)-C(3)	126.27(18)
Cl(1)-Ru(1)	2.4385(5)	C(16)-C(3)-C(4)	118.14(18)
Ru(1)-C(17)	1.808(2)	C(16)-C(3)-C(2)	119.59(18)
Ru(1)-C(1)	1.9898(19)	C(4)-C(3)-C(2)	122.04(18)
Ru(1)-P(2)	2.3964(5)	C(5)-C(4)-C(3)	120.08(19)
Ru(1)-P(1)	2.3969(5)	C(4)-C(5)-C(6)	121.88(19)
P(1)-C(21)	1.849(2)	C(4)-C(5)-H(5)	119.1
P(1)-C(24)	1.850(2)	C(6)-C(5)-H(5)	119.1
P(1)-C(18)	1.869(2)	C(5)-C(6)-C(15)	119.16(19)
P(2)-C(27)	1.842(2)	C(5)-C(6)-C(7)	120.4(2)
P(2)-C(33)	1.854(2)	C(15)-C(6)-C(7)	120.2(2)
P(2)-C(30)	1.858(2)	C(8)-C(7)-C(6)	120.2(2)
O(1)-C(17)	1.159(2)	C(7)-C(8)-C(9)	121.4(2)
C(1)-C(2)	1.332(3)	C(14)-C(9)-C(8)	120.3(2)
C(2)-C(3)	1.474(3)	C(14)-C(9)-C(10)	119.5(3)
C(3)-C(16)	1.380(3)	C(8)-C(9)-C(10)	120.0(2)
C(3)-C(4)	1.417(3)	C(11)-C(10)-C(9)	120.5(3)
C(4)-C(5)	1.364(3)	C(10)-C(11)-C(12)	121.3(2)
C(5)-C(6)	1.408(3)	C(13)-C(12)-C(11)	119.16(17)
C(5)-H(5)	0.9500	C(13)-C(12)-C(11)#1	119.16(17)
C(6)-C(15)	1.415(3)	C(11)-C(12)-C(11)#1	121.7(3)
C(6)-C(7)	1.430(3)	C(12)-C(13)-C(14)#1	117.17(13)
C(7)-C(8)	1.344(3)	C(12)-C(13)-C(14)	117.17(13)
C(8)-C(9)	1.422(4)	C(14)#1-C(13)-C(14)	125.7(3)
C(9)-C(14)	1.415(3)	C(9)-C(14)-C(13)	118.3(2)
C(9)-C(10)	1.423(3)	C(9)-C(14)-C(15)	117.5(2)
C(10)-C(11)	1.340(4)	C(13)-C(14)-C(15)	123.70(19)
C(11)-C(12)	1.425(3)	C(16)-C(15)-C(6)	117.45(18)
C(12)-C(13)	1.417(4)	C(16)-C(15)-C(14)	123.25(19)
C(12)-C(11)#1	1.425(3)	C(6)-C(15)-C(14)	118.91(19)
C(13)-C(14)#1	1.449(3)	C(3)-C(16)-C(15)	123.16(19)
C(13)-C(14)	1.449(3)	O(1)-C(17)-Ru(1)	179.04(18)
C(14)-C(15)	1.456(3)	C(20)-C(18)-C(19)	110.0(2)
C(15)-C(16)	1.409(3)	C(20)-C(18)-P(1)	116.47(17)
C(18)-C(20)	1.518(3)	C(19)-C(18)-P(1)	113.18(17)
C(18)-C(19)	1.522(3)	C(22)-C(21)-C(23)	111.79(18)
C(21)-C(22)	1.529(3)	C(22)-C(21)-P(1)	114.80(15)
C(21)-C(23)	1.533(3)	C(23)-C(21)-P(1)	114.52(16)
C(24)-C(25)	1.520(3)	C(25)-C(24)-C(26)	109.86(19)
C(24)-C(26)	1.541(3)	C(25)-C(24)-P(1)	112.79(16)
C(27)-C(29)	1.525(3)	C(26)-C(24)-P(1)	110.44(15)
C(27)-C(28)	1.527(4)	C(29)-C(27)-C(28)	110.0(2)
C(30)-C(31)	1.526(3)	C(29)-C(27)-P(2)	116.39(16)
C(30)-C(32)	1.542(4)	C(28)-C(27)-P(2)	112.60(17)
C(33)-C(35)	1.524(3)	C(31)-C(30)-C(32)	109.5(2)
C(33)-C(34)	1.529(3)	C(31)-C(30)-P(2)	111.40(16)
		C(32)-C(30)-P(2)	111.97(17)
Cl(3)-C(41)-Cl(2)	111.36(14)	C(35)-C(33)-C(34)	110.01(19)
Cl(5)-C(42)-Cl(4)	111.76(14)	C(35)-C(33)-P(2)	112.80(15)
C(17)-Ru(1)-C(1)	88.86(8)	C(34)-C(33)-P(2)	116.91(17)
C(17)-Ru(1)-P(2)	88.20(6)		
C(1)-Ru(1)-P(2)	99.89(6)		
C(17)-Ru(1)-P(1)	89.85(6)		
C(1)-Ru(1)-P(1)	91.20(6)		
P(2)-Ru(1)-P(1)	168.695(19)		
C(17)-Ru(1)-Cl(1)	173.44(6)		
C(1)-Ru(1)-Cl(1)	97.70(6)		
P(2)-Ru(1)-Cl(1)	90.675(19)		
P(1)-Ru(1)-Cl(1)	89.997(18)		
C(21)-P(1)-C(24)	102.35(10)		
C(21)-P(1)-C(18)	110.16(10)		
C(24)-P(1)-C(18)	103.55(11)		
C(21)-P(1)-Ru(1)	116.99(7)		
C(24)-P(1)-Ru(1)	107.75(7)		
C(18)-P(1)-Ru(1)	114.38(8)		
C(27)-P(2)-C(33)	110.67(11)		
C(27)-P(2)-C(30)	103.93(11)		
C(33)-P(2)-C(30)	102.82(10)		
C(27)-P(2)-Ru(1)	115.66(7)		

Figure S7. Two views of complex **2b**

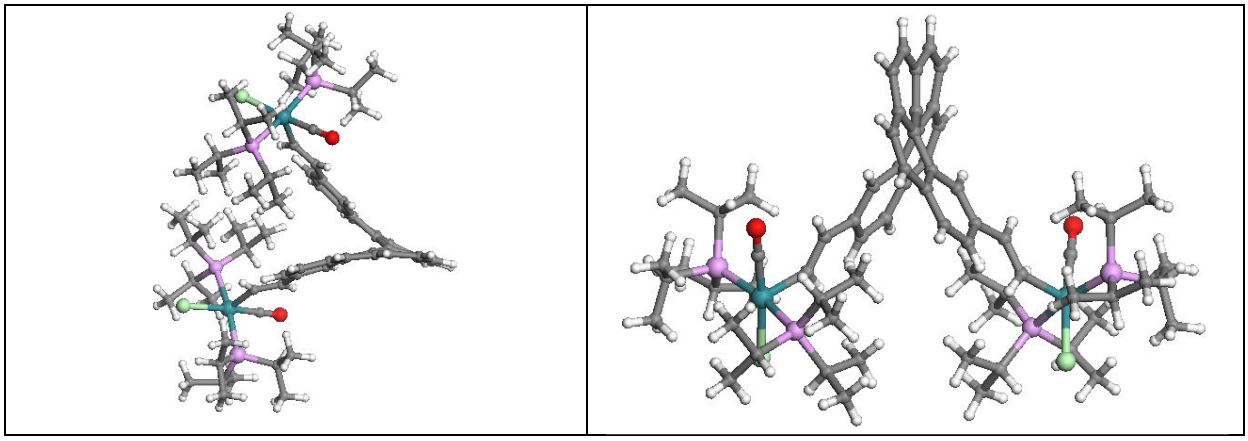

HPLC separation studies

Analytical chiral HPLC separation for compound **1a**

• The sample is dissolved in ethanol, injected on the chiral column, and detected with an UV detector at 254 nm and CD 254nm. The flow-rate is 1 ml/min.

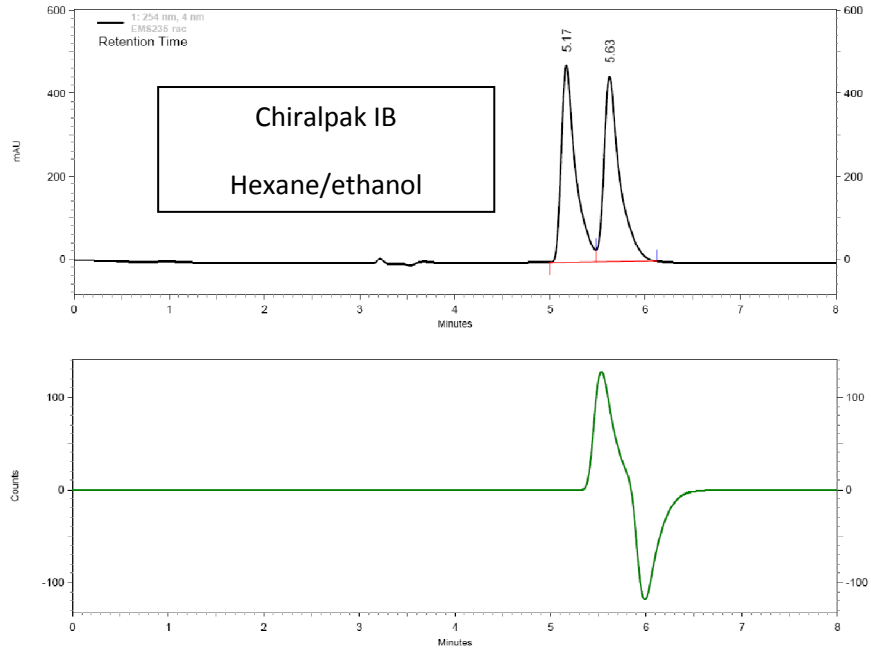

1: 254 nm, 4 nm
Results

Retention Time	Area	Area %	Capacity factor	Relative RT	Resolution (USP)
5.17	20068096	49.12	0.72	1.00	0.00
5.63	20788311	50.88	0.88	1.21	1.69
Totals	40856407	100.00			

Semi-preparative separation for compound **1a** :

• Sample preparation: About 300 mg of compound **1a** are dissolved in 104 mL of a mixture chloroform/ethanol (1/1).
• Chromatographic conditions: Chiralpak IB (250 x 10 mm), thermostated at 30°C, hexane/ethanol (95/5) as mobile phase, flow-rate = 5 mL/min, UV detection at 254 nm.
• Injection (stacked injections): 1300 times 80 µl, every 2.3 minutes.
• Collection: the first eluted enantiomer is collected between 0.2 and 1 minutes and the second one between 1.25 and 2.2 minutes.
• First fraction: 143 mg of the first eluted ((+, CD 254nm)-enantiomer)
• Second fraction: 125 mg of the second eluted ((-, CD 254nm)-enantiomer)
• Chromatograms of the collected enantiomers: UV and CD detections (254nm)

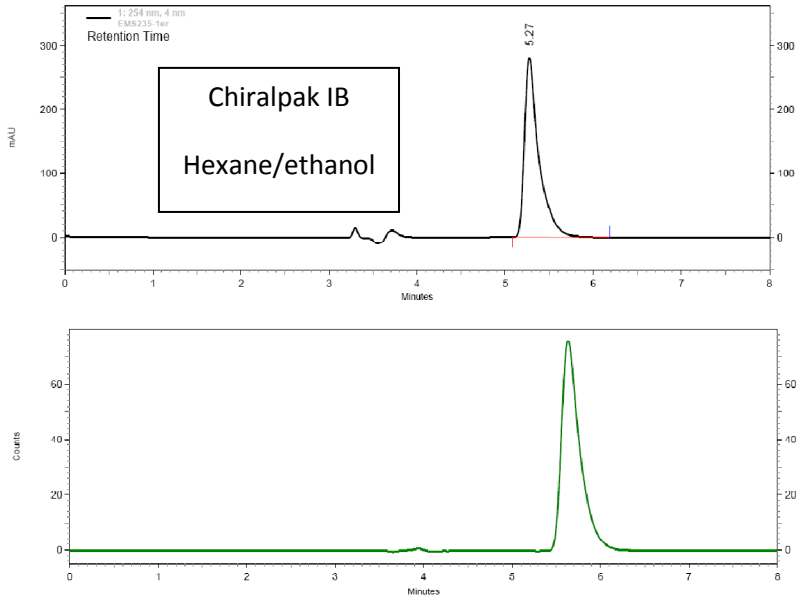

1: 254 nm, 4 nm
Results

Retention Time	Area	Area %	Capacity factor	Relative RT	Resolution (USP)
5.27	12655376	100.00	0.76	1.00	0.00
Totals	12655376	100.00			

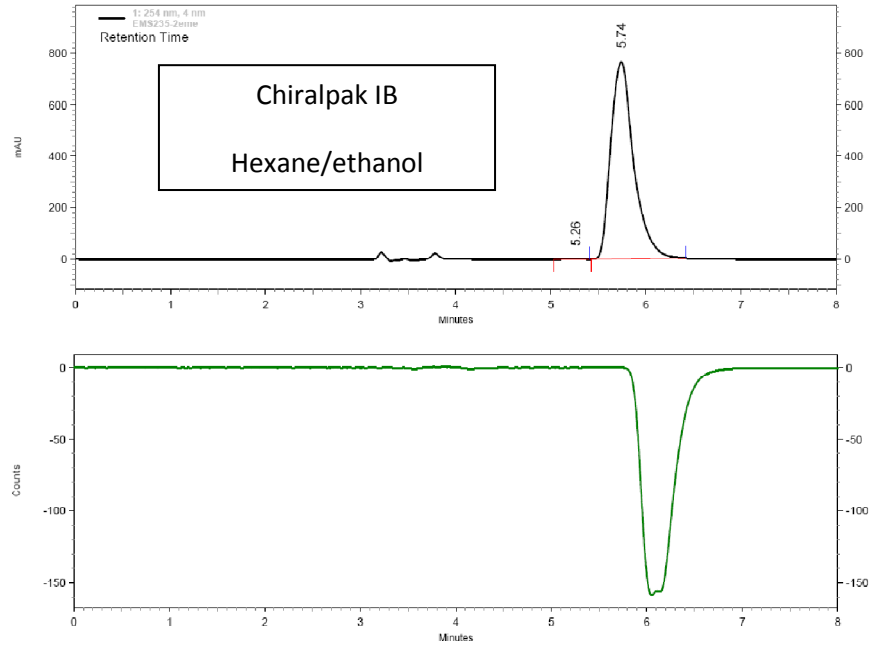

1: 254 nm, 4 nm
Results

Retention Time	Area	Area %	Capacity factor	Relative RT	Resolution (USP)
5.26	21363	0.04	0.75	1.00	0.00
5.74	51427058	99.96	0.91	1.21	1.26
Totals	51448421	100.00			

Analytical chiral HPLC separation for compound**1b**

• The sample is dissolved in ethanol, injected on the chiral column, and detected with an UV detector at 254 nm and a polarimeter. The flow-rate is 1 ml/min.

Column	Mobile Phase	t1	k1	t2	k2	α	Rs
Chiralpak IA	Hexane/ethanol 90/10	5.97	0.99			1	0
Chiralpak IB	Hexane/isopropanol 90/10	5.79 (+)	0.93	6.31 (-)	1.10	1.19	1.21
Chiralpak IC	Hexane/isopropanol 90/10	4.53 (+)	0.51	4.68 (-)	0.56	1.10	0.50
Chiralpak ID	Hexane/isopropanol 90/10	5.19 (+)	0.73	5.36 (-)	0.79	1.08	0.67
Whelk-O1 (*S,S*)	Hexane/isopropanol 90/10	9.23 (+)	2.08	10.75 (-)	2.58	1.24	3.08

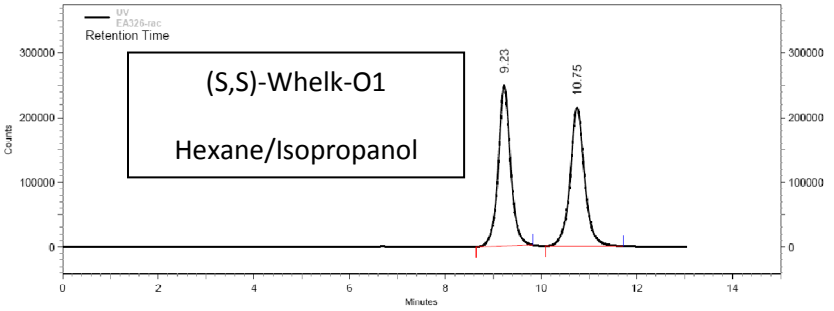

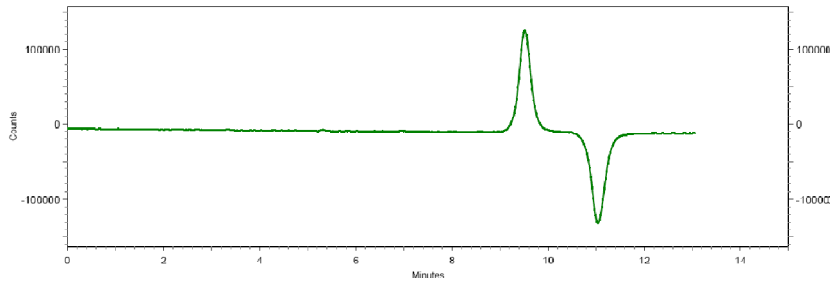

UV Results

Retention Time	Area	Area %	Capacity factor	Relative RT	Resolution (USP)
9.23	4448834	49.75	2.08	1.00	0.00
10.75	4494079	50.25	2.58	1.24	3.08
Totals	8942913	100.00			

Semi-preparative separation for compound **1b** :

• Sample preparation: About 80 mg of compound **1b** are dissolved in 9.3 ml of chloroform.

• Chromatographic conditions: (*S,S*)-Whelk-O1 (250 x 10 mm), thermostated at 30°C, hexane/isopropanol (90/10) as mobile phase, flow-rate = 5 ml/min, UV detection at 370 nm.

• Injection (stacked injections): 62 times 150 µl, every 2 minutes.

• Collection: the first eluted enantiomer is collected between 6.5 and 7.3 minutes and the second one between 7.5 and 8.4 minutes.

• First fraction: 38 mg of the first eluted ((+)-enantiomer)

• Second fraction: 38 mg of the second eluted ((-)-enantiomer)

• Chromatograms of the collected enantiomers: UV and Polarimeter detections

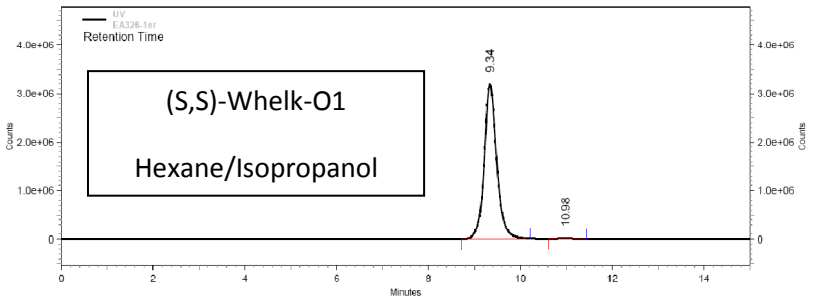

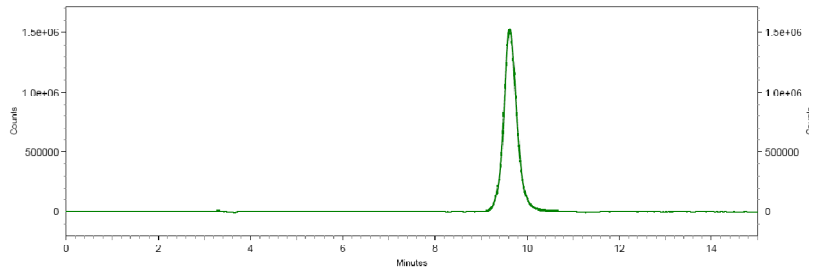

UV Results

Retention Time	Area	Area %	Capacity factor	Relative RT	Resolution (USP)
9.34	60605904	99.62	2.11	1.00	0.00
10.98	230087	0.38	2.66	1.26	3.35
Totals	60835991	100.00			

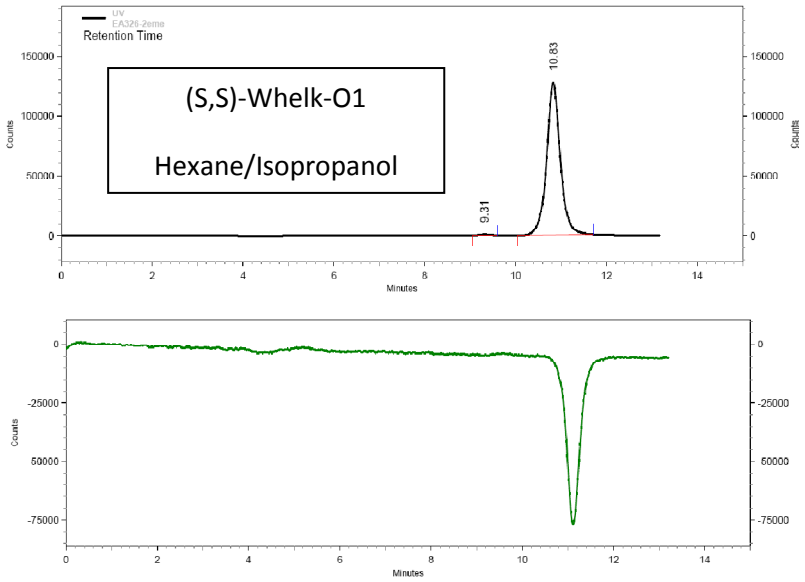

UV Results

Retention Time	Area	Area %	Capacity factor	Relative RT	Resolution (USP)
9.31	13467	0.50	2.10	1.00	0.00
10.83	2683511	99.50	2.61	1.24	3.22
Totals	2696978	100.00			

Table S5. Experimental specific and molar rotations and calculated molar rotations of enantiopure mono and bis-substituted [6]helicene-ethynyl *P*-**1a**,**b** and [6]helicene-vinyl-Ru derivatives *P*-**2a** (monosubstituted) and *P*-**2b** (disubstituted) and of the parent carbo[6]helicene.

	1a	**1b**	**2a**	**2b**
$[\alpha]_D^{23}$ [a,b]	3133	5180	2850	2909
$[\phi]_D^{23}$ [a,c]	11030	20000	23770	39150
$[\phi]$ [d]	17002 (12662)[e]	22230	20583	46076

[a] Measured in CH_2Cl_2. Concentrations: 1-5 10^{-5} M. Error of 5-10%. [b] In deg/[dm (g/cm^{-3})]. [c] In deg cm^2 dmol^{-1}. [d] BHLYP/SV(P) calculations using the *P* enantiomers optimized with BP/SV(P). [e] Obtained with the geometry from the X-ray diffraction study.

Electrochemistry / Spectroelectrochemistry

General Comments. Electrochemical studies were carried out under argon using an Eco ChemieAutolab PGSTAT 30 potentiostat (CH_2Cl_2, 0.0.2M Bu_4NPF_6), the working electrode was a Pt disk, and ferrocene the internal reference. UV/Vis/NIR spectroelectrochemistry (SEC) experiments were performed at 20 °C, under argon, with a home-made Optically Transparent Thin-Layer Electrosynthetic (OTTLE) cell, , using a Varian CARY 5000 spectrometer and an EG&G PAR model 362 potentiostat. A Pt mesh was used as the working electrode, a Pt wire as the counter electrode, and a Pt wire as a pseudo-reference electrode. The electrodes were arranged in the cell such that the Pt mesh was in the optical path of the quartz cell. The anhydrous freeze-pump-thaw degassed sample-electrolyte solution (0.2 M *n*-Bu_4NPF_6) was cannula-transferred under argon into the cell previously thoroughly deoxygenated. Stable isobestic points were observed during oxidation or reduction. In every case re-reduced or re-oxidized samples displayed in the spectral region of interest no features other than those of the parent material. IR experiments were performed in similar conditions using a modified cell with KBr windows, on a Jasco FVS-6000 spectrometer.

Cyclic voltammetry on complex 2a

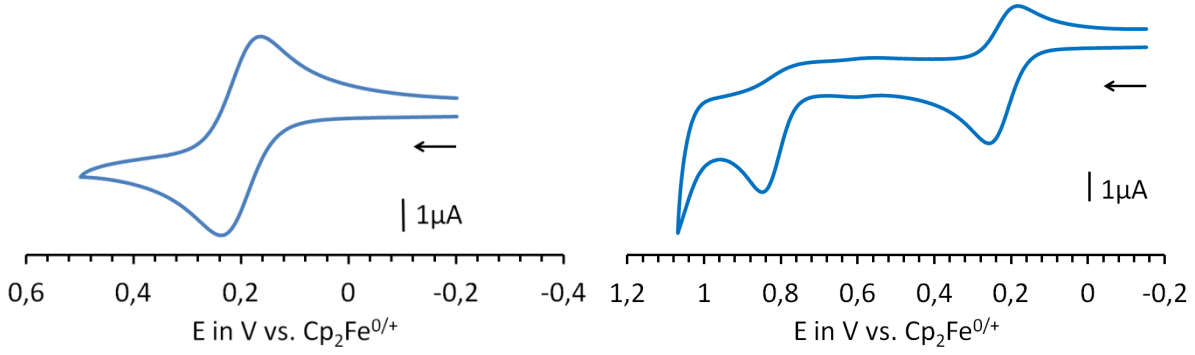

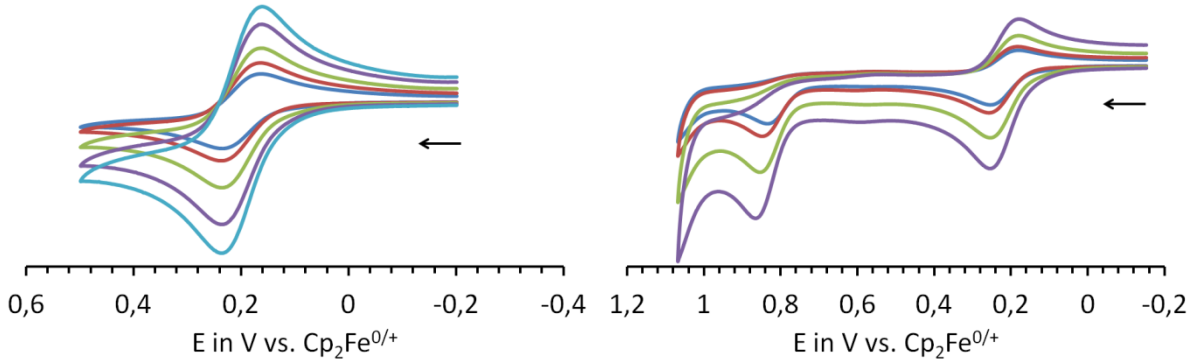

Figure S8. Voltammetric scans of complex **2a** in CH_2Cl_2/NBu_4PF_6 (O.2M) at r.t. Upper curves: scans at V=0.1 V/s; lower graphs: V=0.05, 0.1, 0.2, 0.4 and 0.6 V/s.

Cyclic voltammetry on complex 2b

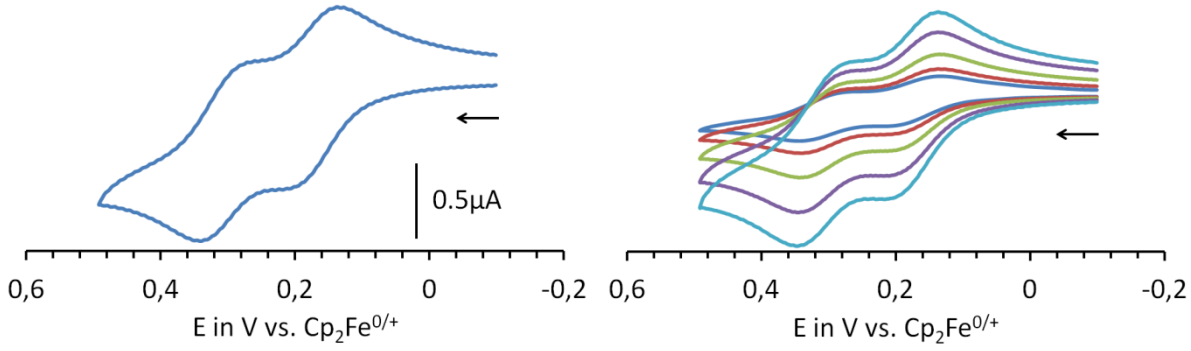

Figure S9. Voltammetric scans of complex **2b** in CH_2Cl_2/NBu_4PF_6 (0.2M) at r.t. Left curves: scans at V=0.1 V/s; right graphs: V=0.05, 0.1, 0.2, 0.4 and 0.6 V/s.

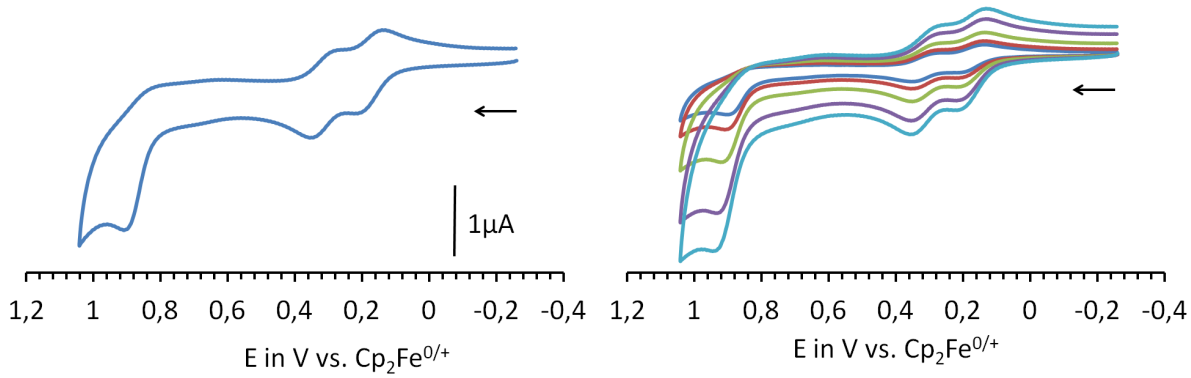

Figure S10. Voltammetric scans of complex **2b** in CH_2Cl_2/NBu_4PF_6 (0.2M) at r.t.. Left curves: scan at V=0.1 V/s; right graph: V=0.05, 0.1, 0.2, 0.4 and 0.6 V/s.

Table S6. Electrochemical data of complexes **2a**, **2b**.[a,b]

	$E_{1/2}^{0/+}$ (V)	$E_{1/2}^{+/2+}$ (V)	$E_{1/2}^{2+/3+}$ (V)
2a	0.173	0.781[c]	
2b	0.146	0.285	0.830[c]

[a] Data in CH_2Cl_2 / 0.2 M NBu_4PF_6 at room temperature. [b] Potentials are calibrated against the internal Fc/Fc^+couple which is set as 0.00 V. [c] Peak potential of an irreversible process at V (0.1 V/s).

Figure S11. IR spectroelectrochemistry: oxidation of complex **2a** in DCE/ 0.2 M NBu_4PF_6 at r.t.

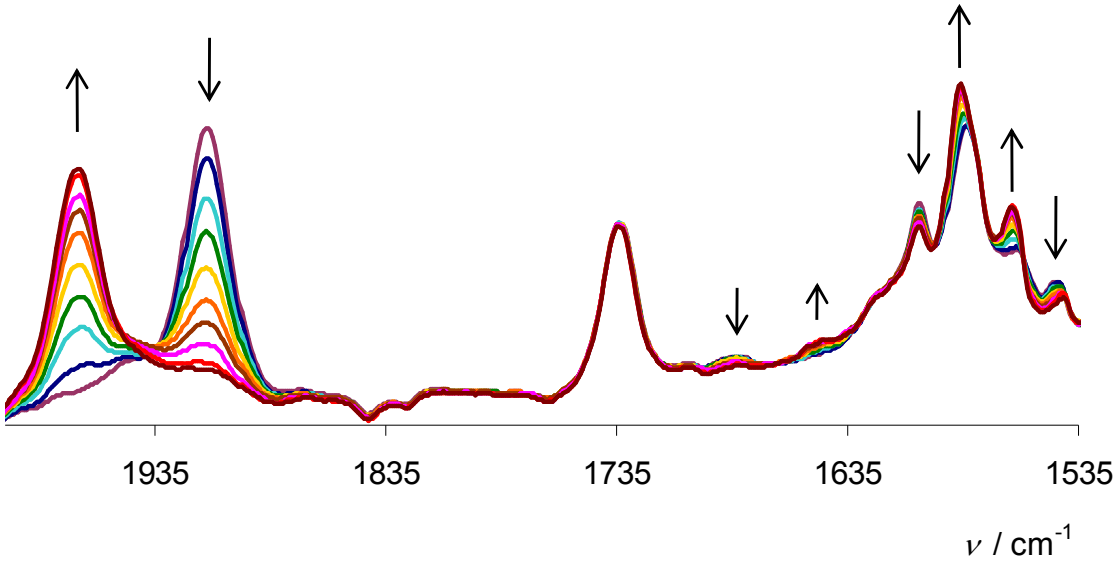

Figure S12. IR spectroelectrochemistry: first oxidation of complex **2b** in DCE/0.2 M NBu_4PF_6 at r.t.

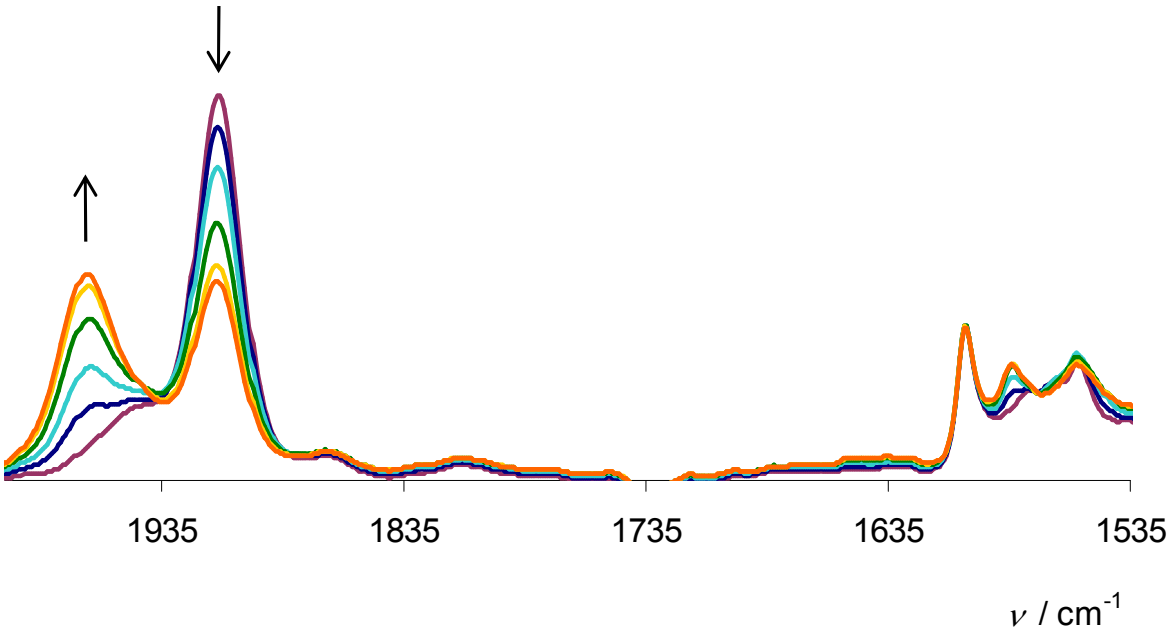

Figure S13.IR spectroelectrochemistry: second oxidation of complex **2b**in DCE/0.2 M NBu_4PF_6 at r.t.

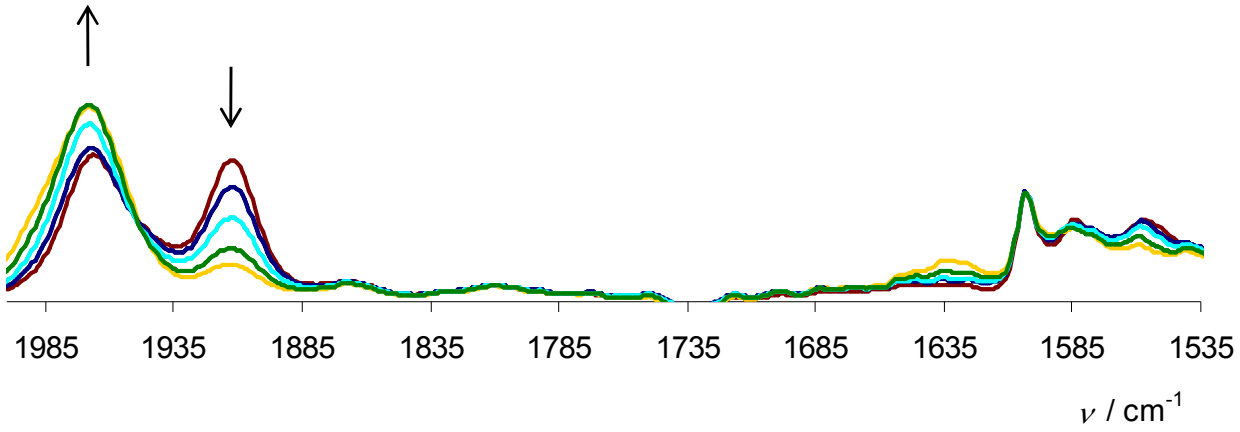

Figure S14. UV/Vis/NIR spectroelectrochemistry: oxidation at 0.4V (*vs.* Fc/Fc^+) of complex **2a** in DCE/0.2 M NBu_4PF_6 at r.t., followed by reduction at -0.4V (*vs.* Fc/Fc^+)

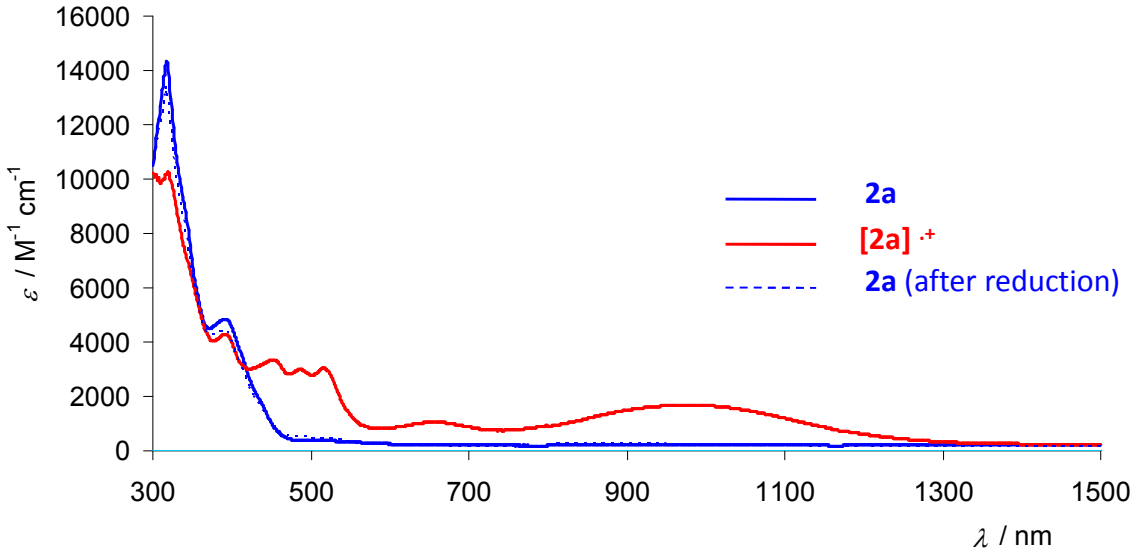

Figure S15. UV: Vis/NIR spectroelectrochemistry: first and second oxidation of complex **2b** in DCE/NBu_4PF_6 at r.t.

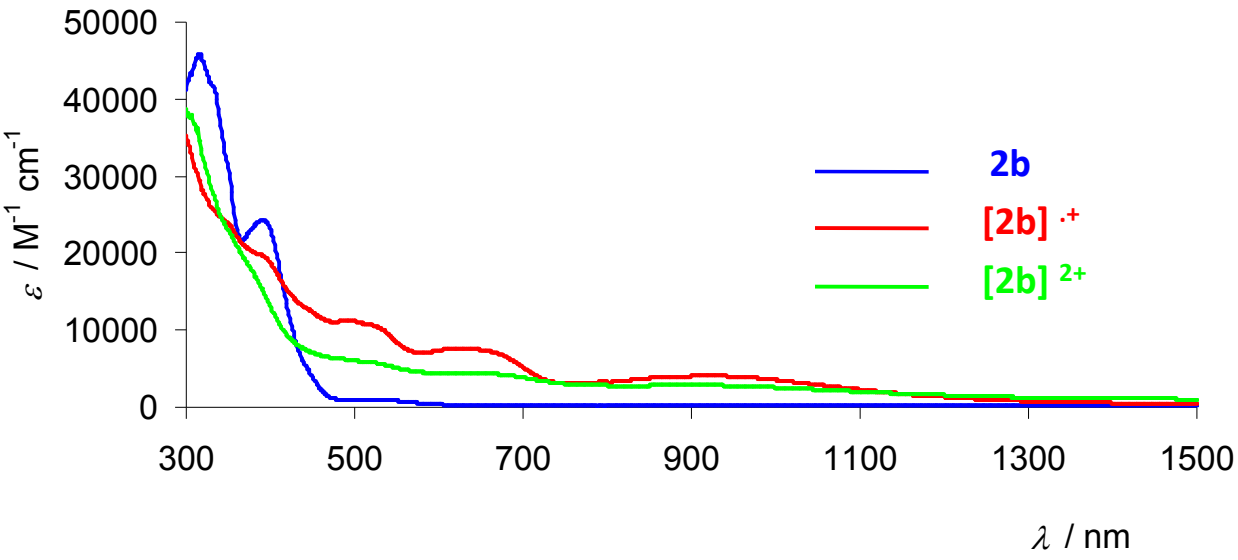

Figure S16. a) CD spectra of *P*-(+)-**2b** (red) and of its oxidized species (blue) in DCE at room temperature, and reduced species (dotted red), showing the reversibility. b) NIR-CD region spectra of *P*-(+)-**2b** (red) and *P*-(-)-[**2a**]$^{\bullet+}$ (blue). c) Redox chiroptical switching *M*-(-)-**2b** <-> [*M*-(-)**2b**]$^{\bullet+}$ observed by CD spectroscopy at 500 nm.

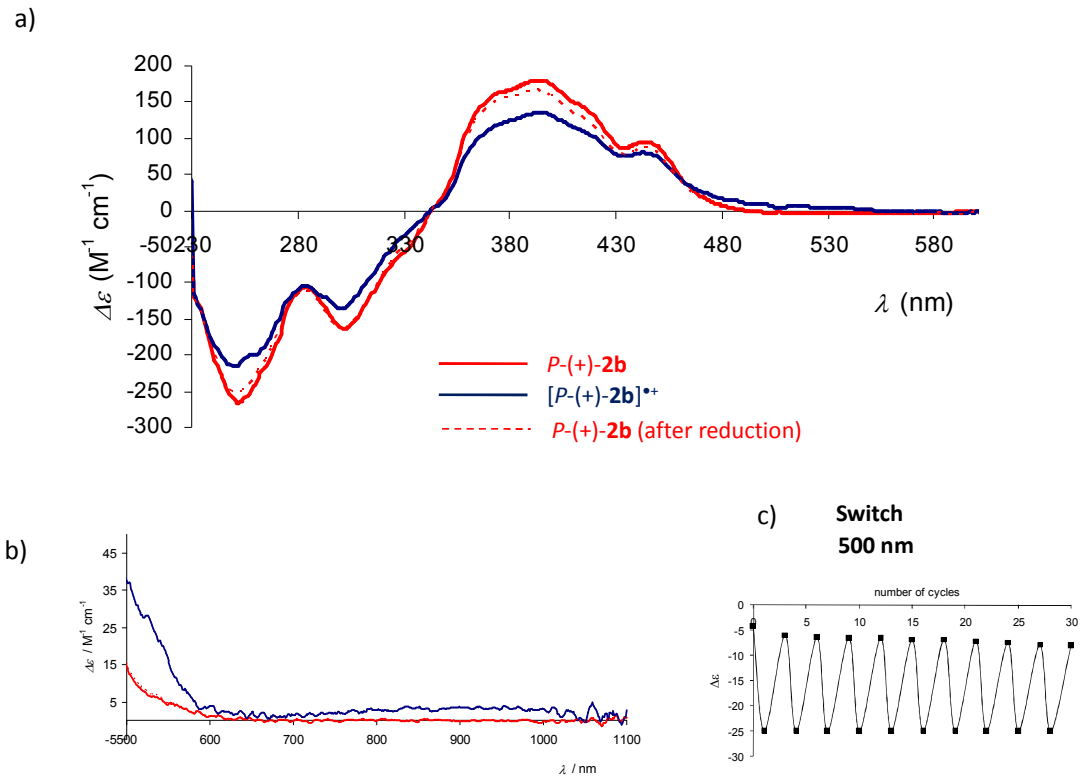

EPR mesasurements.

The EPR spectra were recorded at 77K using a EMX-8/2,7 Brucker spectrometer equipped with a Brucker nitrogen temperature controller ER4131VT02. Prior to recording their EPR spectra, the singly oxidized complexes were chemically generated with $[N(C_6H_4\text{-}4\text{-}Br)_3][SbCl_6]$.[25]

Figure S17. EPR spectrum of $[\mathbf{2a}]^{\bullet+}SbCl_6^-$ in THF at77 K.

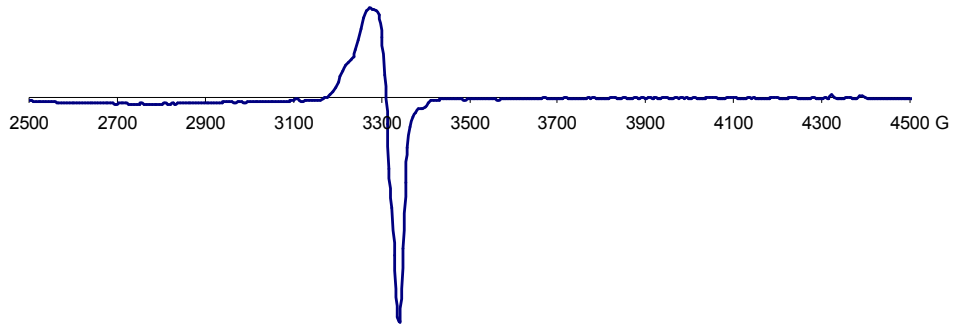

g_x= 2.0225, g_y = 2.0450, g_z = 2.0990 (based on simulation)

Very slightly rhombic EPR signal at 77 K (Δg = 0.076) with $g_{<av>}$ = 2.055.

Figure S18. EPR spectrum of $[\mathbf{2b}]^{\bullet+}SbCl_6^-$ in THF at 77 K.

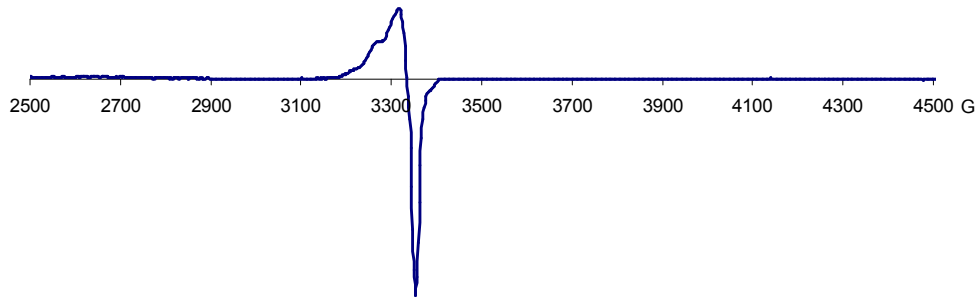

g_x = 2.0205, g_y = 2.0475, g_z = 2.0990 (based on simulation)

Slightly anisotropic EPR signal at 77 K (Δg = 0.079) with $g_{<av>}$ = 2.056.

Computational details

All computations were carried out using DFT, with the Turbomole package, version 5.7.1. [10, 11] Geometry optimizations employed the BP functional [12–14] with a standard Turbomole split-valence basis set with one set of polarization functions for non-hydrogen atoms, SV(P), [15, 16] abbreviated as BP/SV(P) in the following. For the Ru atoms, a scalar relativistic effective core potential was used [17]. Optical Rotation (OR) and Circular Dichroism (CD) calculations were performed using Time-Dependent DFT (TDDFT) with the BHLYP functional [18, 19] and the SV(P) basis set. The optical rotation parameters were computed at the sodium D-line wavelength λ = 589.3 nm. The CD calculations reported here cover 120 lowest singlet excited states to assure that all transitions with a significant rotatory strength in the experimentally observed energy range (~ 2.5 – 5.5 eV) are included. The simulated spectra shown are the sums of Gaussian functions centered at the vertical excitation energies and scaled using the calculated rotatory strengths as previously described in Ref. [20]. For the root mean square width, the parameter of σ = 0.2 eV was used in all cases. As previous studies showed, the presented above level of methodology is fairly well suited for effective and reasonably accurate description of the chiroptical properties of helicene-metal complexes [21, 22]. The systems studied include ruthenium(II)-grafted vinylhelicene derivatives **2a** (monometallic) and **2b** (bimetallic) together with the free ligands (**1a** and **1b**). Additional B3LYP/SV(P) [12, 18, 23, 24] computations were performed for the radical cations $[\mathbf{2a}]^{\bullet+}$, $[\mathbf{2b}]^{\bullet+}$, and $[\mathbf{2b}]^{2+}$. The system $[\mathbf{2b}]^{2+}$ was calculated in two spin states, a triplet and an open-shell singlet (the latter approximated by a single-determinant spin unrestricted Kohn-Sham wavefunction with $\langle S_z \rangle = 0$). The energies for the two states were very close (compare Figure S22); thus, within the error bars of the DFT energies and given the approximate form by which the singlet state energy is calculated in DFT [26] we cannot clearly identify which of the species is lower in energy. The calculations indicate that the coupling of the unpaired spins between the two metal centers is relatively weak. All calculations were carried out for the *P*-(+) isomers without imposing symmetry.

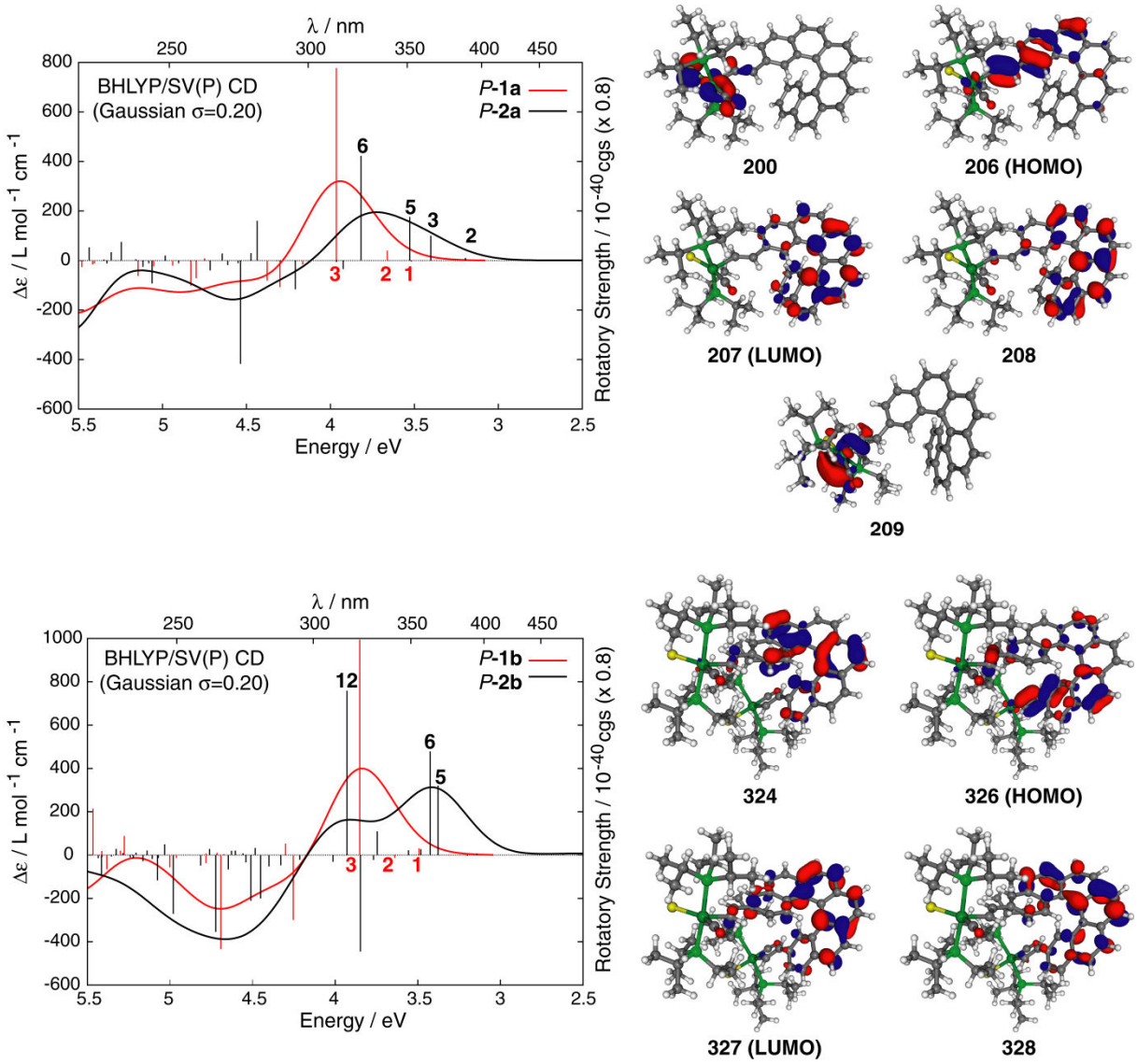

Figure S19. Top: Comparison of the BHLYP/SV(P) TDDFT CD spectra of *P*-**1a** (red line), and *P*-**2a** (black line), and isosurfaces (0.04 au) of MOs involved in selected transitions of **2a**. Bottom: Comparison of the BHLYP/SV(P) TDDFT CD spectra of *P*-**1b** (red line), and *P*-**2b** (black line), and isosurfaces (0.04 au) of MOs involved in selected transitions of **2b.** Numbered excitations correspond to those analyzed in Table S7.

Table S7. Selected intense excitations and molecular orbital (MO) pair contributions (greater than 10%) of *P*-**1a,1b** and *P*-**2a,2b**.

Excitation	*E* / eV	*R* / 10^{-40} cgs	MO(from)	MO(to)	%
		P-**1a**			
#1	3.53	9.36	92	93	42.1
			91	94	26.3
			91	93	10.1
#2	3.66	50.18	91	93	51.3
			92	94	21.9
			92	93	16.2
#3	3.97	971.85	91	94	57.0
			92	93	31.2
		P-**1b**			
#1	3.49	39.25	98	99	55.8
			97	100	30.4
#2	3.64	-16.17	97	99	58.4
			98	100	33.5
#3	3.85	1242.53	97	100	55.9
			98	99	32.9
		P-**2a**			
#2	3.20	13.41	200	209	70.6
#3	3.40	125.60	206	207	64.6
			205	208	14.8
			204	207	10.9
#5	3.53	220.03	206	208	58.1
			205	207	18.7
#6	3.82	528.55	205	207	39.4
			205	208	34.0
		P-**2b**			
#5	3.38	400.73	326	327	64.1
#6	3.43	598.37	326	328	48.1
			325	327	12.4
			324	327	10.5
			326	327	10.0
#12	3.93	948.48	324	327	41.2
			324	328	33.9

Figure S20. Comparison of the experimental (dashed lines) and TDDFT BHLYP/SV(P) (solid lines) CD spectra of *P*-(+)-**1a**, -**1b**, -**2a**, and -**2b**. No spectral shift has been applied.

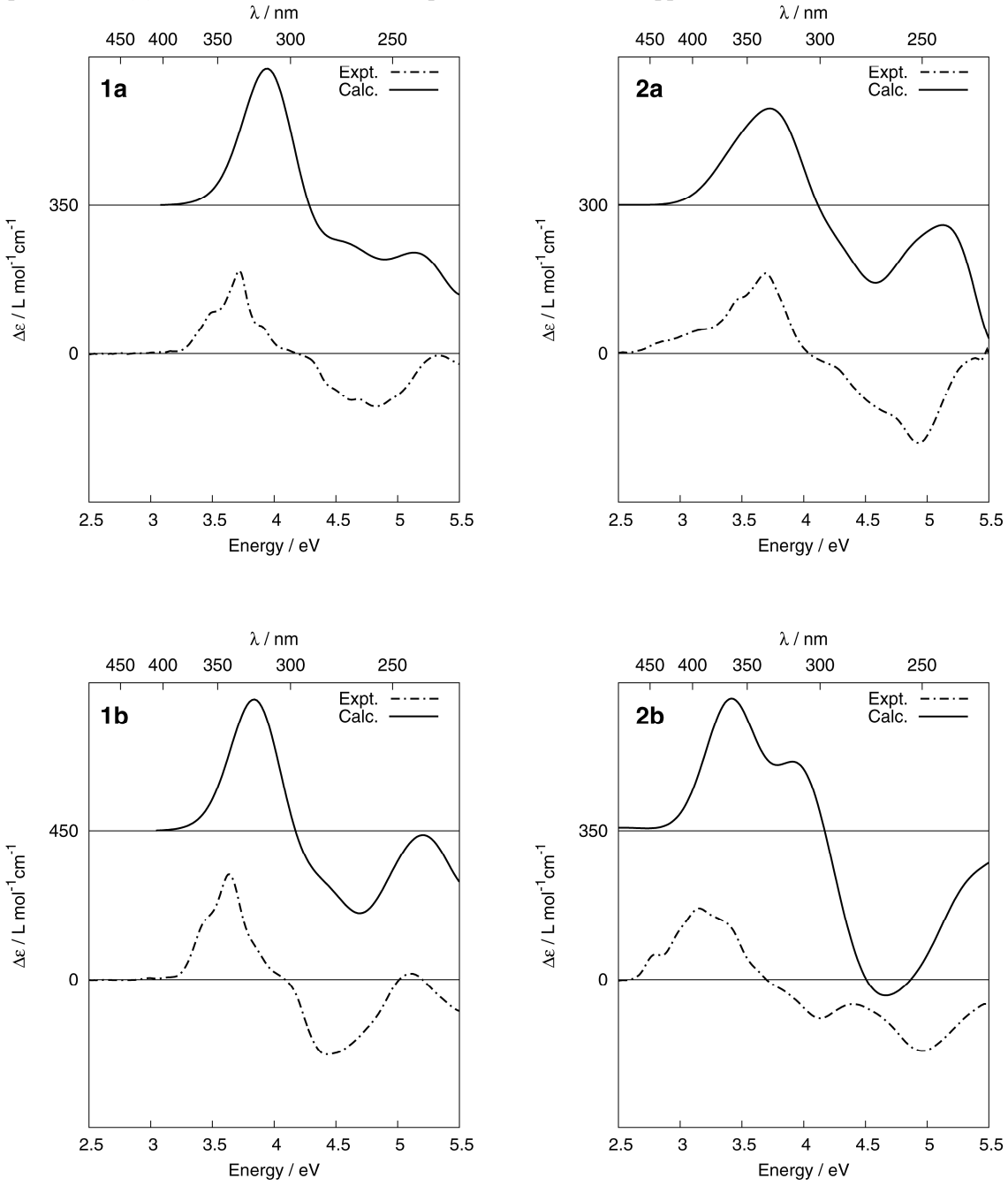

Figure S21. Plots of electron spin density, $\Delta\rho = \rho^{\alpha} - \rho^{\beta}$, (panel **a**) together with the frontier orbitals (panel **b**) in the [**2a**]$^{\bullet+}$ and [**2b**]$^{\bullet+}$ complexes. The contours are 0.05 au for orbitals and 0.005 au (**2a**) / 0.002 au (**2b**) for spin density. Numbers listed are fractions of the total integrated spin density obtained from Mulliken decompositions of $\Delta\rho$.

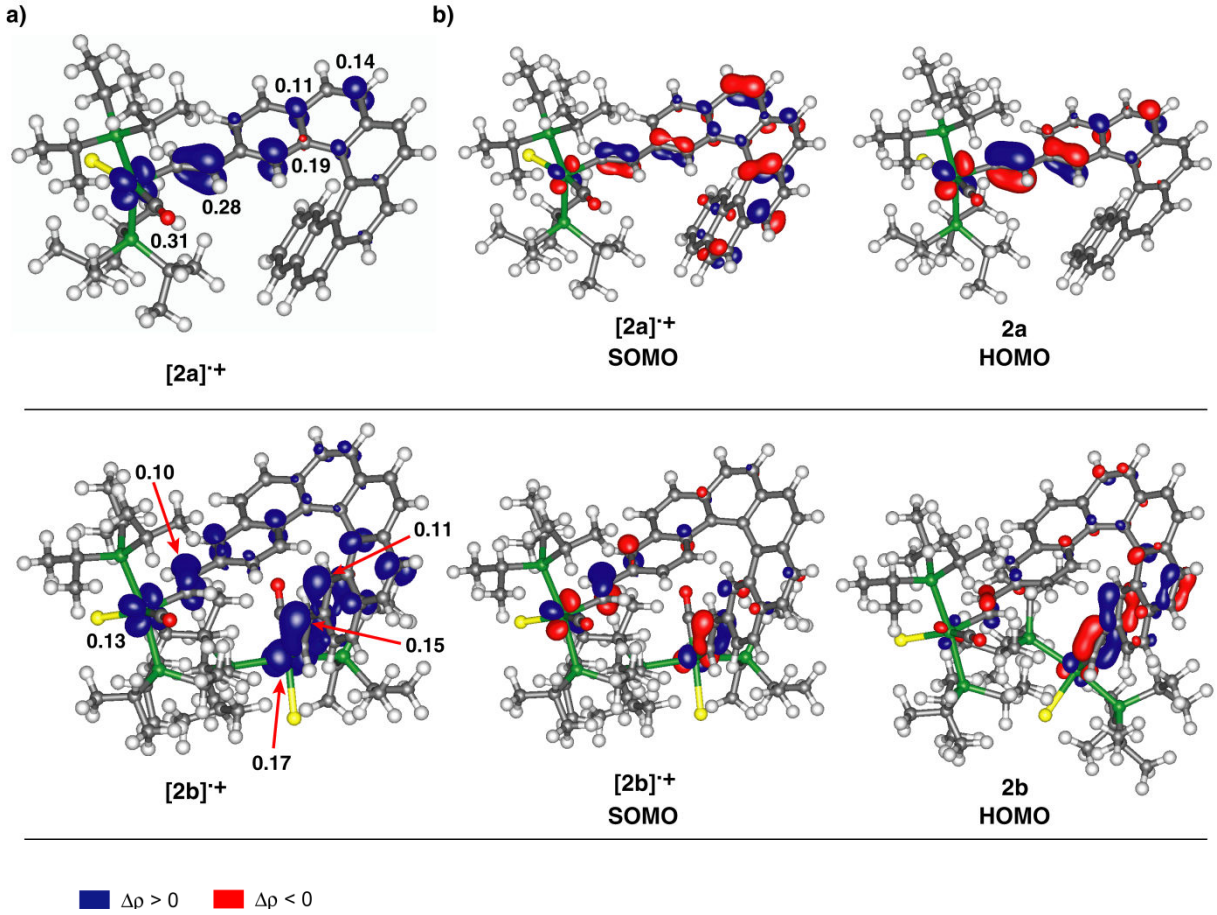

Figure S22. a) Frontier orbitals of triplet-state (S = 1) *P*-[**2b**]$^{2+}$ together with their bonding ('+') and antibonding ('–') combinations. The constant c is 1/√2. b) Frontier orbitals of open-shell singlet-state (S = 0) *P*-[**2b**]$^{2+}$. The contours are 0.03 au.

a) S = 1 (*E* = -27681.48 kcal/mol)

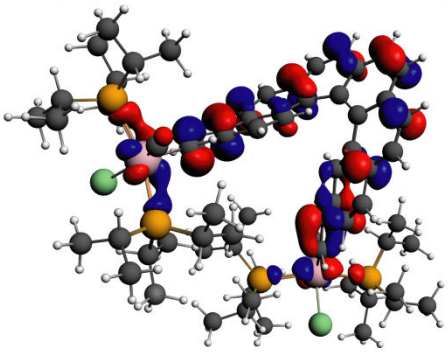

α(SOMO-1)
E = -10.111 eV

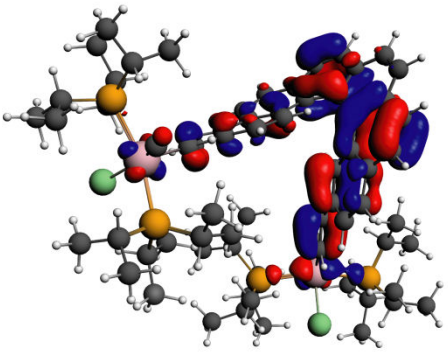

α(SOMO)
E = -9.943 eV

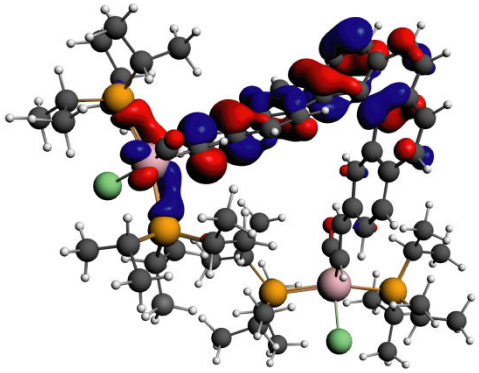

c[α(SOMO)+α(SOMO-1)]

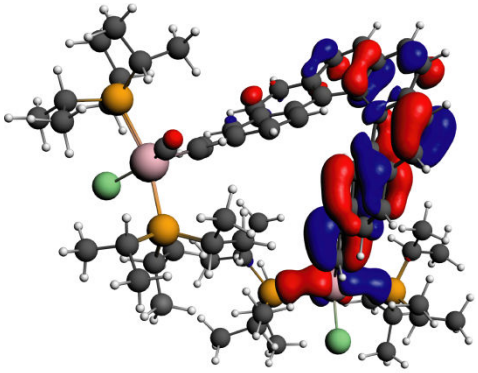

c[α(SOMO)-α(SOMO-1)]

b) S = 0 (*E* = -27681.64 kcal/mol)

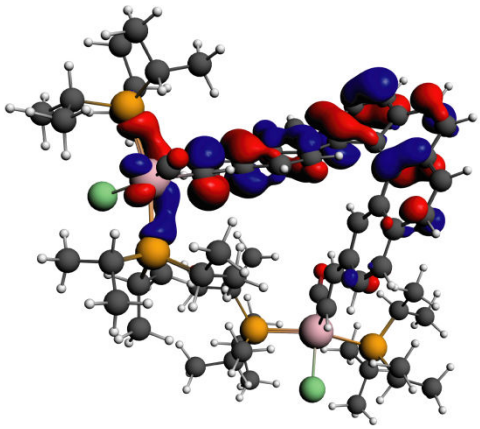

α(SOMO)
E = -10.032 eV

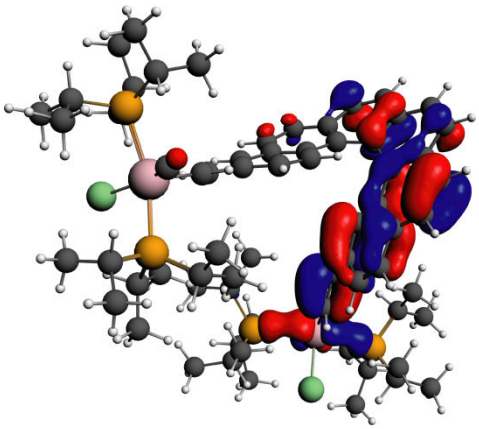

β(SOMO)
E = -9.999 eV

Figure S23. Isosurfaces (0.04 au) of MOs involved in selected transitions of *P*-(+)-**1a** (panel **a**) and -**1b** (panel **b**).

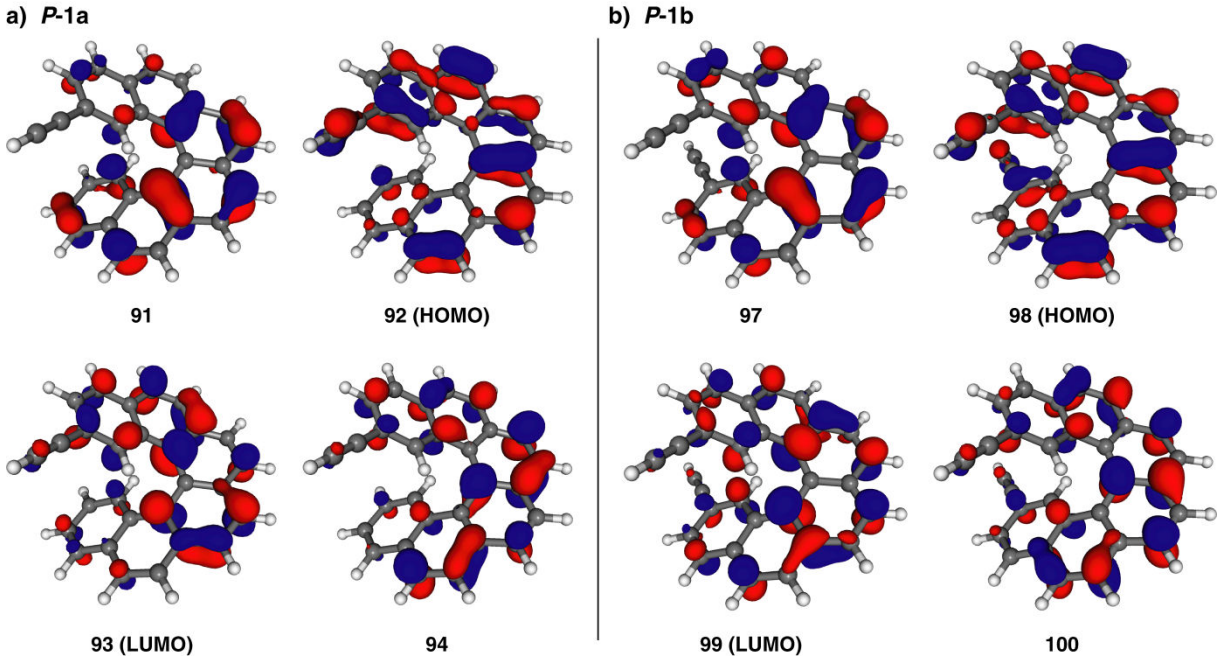

[1] Lightner, D.A.; Powers, T. W.; Frank, G. W.; Trueblood, K. N.; Hefelfinger, D. T. *J. Am. Chem. Soc.* **1972**, *94*, 3492-3497.

[2] Terfort, A.; Görls, H.; Brunner, H. *Synthesis***1997**, *1*, 79-86.

[3] Austin, B.W.; Bilow, N.; Kelleghan, W.J.; Lau, K.S.Y. *J. Org. Chem.* **1981**, *46*, 2280-2286.

[4] Esteruelas, M.A.; Werner, H. *J. Organometal. Chem.* **1986**, *303*, 221-231.

[5] Fox, J. M.; Lin, D.; Itagaki, Y.; Fujita, T. *J. Org. Chem*. **1998**, *63*, 2031-2038.

[6] Otwinowski, Z.; Minor, W. in *Methods in Enzymology*, (Ed.: C.W. Carter, Jr. & R.M. Sweet), New York: Academic Press, **1997**, 276, 307.

[7] Altomare, A.; Burla, M. C.; Camalli, M.; Cascarano, G.; Giacovazzo, C.; Guagliardi, A.; Moliterni, A.G.G.; Polidori, G.; Spagna, R. *J. of Applied Cryst.* **1999***, 32,* 115.

[8] Sheldrick G.M., *SHELX97,* Program for the Refinement of Crystal Structures, University of Göttingen, Germany, **1997**.

[9] International Tables for X-ray Crystallography, vol C, Ed. Kluwer, Dordrech, **1992**.

[10] TURBOMOLE V5.7.1, Quantum Chemistry Group, University of Karlsruhe, Germany, **2005**.

[11] Ahlrichs, R.; Bär, M.; Häser, M.; Horn, H.; Kölmel, C. *Chem. Phys. Lett.* **1989**, *162*, 165-169.

[12] Becke, A. D. *Phys. Rev. A* **1988**, 38, 3098-3100.

[13] Perdew, J. P. *Phys. Rev. B* **1986**, *33*, 8822-8824.

[14] Perdew, J. P. *Phys. Rev. B* **1986***, 34,* 7406.

[15] Schäfer, A.; Horn, H.; Ahlrichs, R. *J. Chem. Phys.* **1992**, *97*, 2571-2577.

[16] Eichkorn, K.; Weigend, F.; Treutler, O.; Ahlrichs, R. *Theor. Chem. Acc.* **1997**, *97*, 119-124.

[17] Andrae, D.; Häußermann, U.; Dolg, M.; Stoll, H; Preuß, H. *Theoret. Chim. Acta* **1990**, *77*, 123-141.

[18] Lee, C.; Yang, W.; Parr, R. G. *Phys. Rev. B* **1988**, *37*, 785-789.

[19] Becke, A. D. *J. Chem. Phys.* **1993**, *98*, 1372-1377.

[20] Autschbach, J.; Ziegler, T.; van Gisbergen, S. J. A.; Baerends, E. J. *J. Chem. Phys.* **2002**, *116*, 6930-6940.

[21] Graule, S.; Rudolph, M.; Vanthuyne, N.; Autschbach, J.; Roussel, C.; Crassous, J.; Réau, R. *J. Am. Chem. Soc.* **2009**, *131*, 3183-3185.

[22] Norel, L.; Rudolph, M.; Vanthuyne, N.; Williams, J. A. G.; Lescop, C.; Roussel, C.; Autschbach, J.; Crassous, J.; Réau, R. *Angew. Chem. Int. Ed.* **2010**, *49*, 99-102.
[23] Vosko, S.; Wilk, L.;Nusair, M. *Can. J. Phys.* **1980**, *58*, 1200-1211.
[24] Stephens, P. J.; Devlin, F. J.; Chabalowski, C. F.; Frisch, M. J. *J. Phys. Chem.* **1994**, *98*, 11623-11627.
[25] Connelly, N. G; Geiger, W. E. *Chem. Rev.* **1996**, *96*, 877-910.
[26] Ziegler, T.; Rauk, A.; Baerends, E. J. *Theoret. Chim. Acta* **1977**, *43*, 261-271.